IEEE Access
Multidisciplinary | Rapid Review | Open Access Journal

Received July 21, 2019, accepted August 23, 2019, date of publication September 4, 2019, date of current version September 25, 2019.

Digital Object Identifier 10.1109/ACCESS.2019.2939491

From Studying Real Hummingbirds to Designing Hummingbird-Like Robots–A Literature Review

YANGHAI NAN[1,2,3], BEI PENG[1,2], YI CHEN[4], (Senior Member, IEEE), AND DON MCGLINCHEY[3]

[1]School of Mechanical and Electrical Engineering, University of Electronic Science and Technology of China, Chengdu 611731, China
[2]Center for Robotics, University of Electronic Science and Technology of China, Chengdu 611731, China
[3]School of Engineering and Built Environment, Glasgow Caledonian University, Glasgow G4 0BA, U.K.
[4]School of Engineering, Newcastle University, Newcastle upon Tyne NE1 7RU, U.K.

Corresponding authors: Bei Peng (beipeng@uestc.edu.cn) and Yi Chen (leo.chen@ieee.org)

This work was supported in part by the National Natural Science Foundation of China under Grant 51575090 and Grant 51975107, in part by the Artigent Young Talent Scholarship Award under Grant 2015001, in part by the Dean's Scholarships for International Academic Excellence under Grant 20170001, and in part by the School of Engineering and Built Environment, Glasgow Caledonian University.

ABSTRACT In this paper, the interpretation of hovering flight for hummingbirds is studied from a hummingbird morphology perspective (muscle and skeleton) including weight distribution, followed by a discussion of hovering aerodynamics. Next, by studying the scale laws, geometry similarity, and statistical analysis on wing parameters, the parametric relation between wing performances and weight is studied, followed by flapping wing micro autonomous drones (FWMADs) design. The efficiency of the designed wings based on the scaling law is verified by flying test. Material difference and methods of design are summarized. Last, the morphology of bird's tails is presented, and then the designs of tails are introduced, followed by discussion of tail performances. The results show that the tail could be predicted to apply to the stability of hovering twin-wing FWMADs. The current studies provide a simple but powerful guideline for biologists and engineers who study the morphology of hummingbirds and design FWMADs.

INDEX TERMS Hummingbird morphology, hovering flapping flight, FWMAD, bio-inspired fabrication, weight distribution, wing design.

I. INTRODUCTION

Hummingbirds are one of the few extensively studied vertebrate species. They fly vocal agile, maneuverable and in particular hovering when feeding at flowers. There are more than 330 species in nature. The smallest one, Bee Hummingbird (Calypte Helenae, from Cuba) is only about 2 grams, whereas the largest one, Giant Hummingbird (PatagonaGigas, from Chile), is almost 20 grams [1]. Their super agility has attracted much attention and currently inspires the development of FWMADs as they are able to perform tasks in a dangerous or inaccessible environment (Due to their small size and hovering feature, it is better than that of Unmanned Aerial Vehicle). The studies show that the aerodynamic efficiency of flapping wings at relatively low speed may be higher than that of a revolving wing at certain low Reynolds number [2], [3]. However, some researchers keep different minds, which have no consensus. Over the last decade, researchers have developed FWMADs inspired by natural flyers such as bee, beetle, dragonfly, butterfly, hummingbird etc. However, insects and hummingbirds have completely different morphology construction although they do not have a dissimilar aerodynamic mechanism.

At present, some researchers analyzed and summarized the current development of FWMADs. Ward *et al.* [4] did the review study of Biomimetic Air Vehicle over the last 30 years (1984 - 2014) from the view of aerodynamics, guidance and control, mechanisms, structure and materials, and system design. The flapping wing micro air vehicle (MAV) modelling was reviewed in paper [5], which introduces the hover capable flapping wing flight in previous work and looks at existing modeling methods used to research the aerodynamics and overall vehicle behavior of a hypothetical MAV. Then Platzer and Jones [6] studied the flapping-wing aerodynamics progress and challenges. The wings of Man-made flyers inspired by the natural flyers were also studied by Rojratsirikul [7]. Additionally, the development of flapping wing MAV in Asia was studied by Tan *et al.* [8]. And Chen C and

The associate editor coordinating the review of this manuscript and approving it for publication was Zhonglai Wang.

Zhang T Y reviewed the design and fabrication of the flapping wing MAV [9]. Floreano D and Wood J R also provided the future development of small autonomous drones [10]. Although maneuvering ability of hummingbird from view of morphology is explained [11], there is no comprehensive summary on hummingbird-like robot from morphology of hummingbird to its robots. Therefore, this paper is useful and meaningful to design and develop hummingbird-like MAV.

In the following subsection, the morphology of insects and flyer robotics inspired by the insects are first introduced. Then, the morphology of birds and flyers robotics inspired by the hummingbird is presented.

A. MORPHOLOGY INTRODUCTION OF INSECTS AND FLYER ROBOTICS INSPIRED BY THE INSECTS

Flying insects and hummingbird have a completely distinct construction of apparatus. Insects have a shell or exoskeleton of highly elastic composition material including chitin microfibers embedded in a protein matrix. The insects' thorax can be regarded as a box combining the sides (pleura) and the base (sternum), and the wings are connected to the side by flexible membranes [12]. There are two ways to produce flapping in insects via direct or indirect muscles [13]. Direct muscles are applied to flap their wings for phylogenetically older insects. There are two groups of muscles, the depressors, and the elevators, which contract to move the wing in upstroke and downstroke separately. Direct drive is typical for four-winged insects like dragonflies. Taking dragonfly as an example, wings are directly linked to large muscles within the flight thorax. Elevators muscles attach to the thorax base and connect to the inner side of a pivoted wing base, whereas depressor muscles connect to the outer side of the pivoted wing base. Therefore, elevators muscles and depressor muscles pull wing up and down flapping separately, shown in Fig. 1-I. Meanwhile, the brain controls each wing independently, which makes very agile flights, but it also restricts their flapping frequency, which is relatively low. The direct muscles of the dragonfly are synchronous muscles.

As for phylogenetically modern insects like flies and bees, dorsoventral and longitudinal muscles are the main flight wing-driven muscles. Vertical muscles (Dorsal ventral) connect from the roof-based thorax, whereas longitudinal muscles (Dorsal longitudinal) connect between the anterior (front) and posterior (back) ends of the thorax. They are activated by stretching and deactivated by shortening. All actuations are carried out through the elaborate wing hinge mechanism at the wing root. It means that they operate their wings by deformation of a thorax or the notum (a dorsal part of the thorax). When contracting vertical muscles and lowering thorax roof down directly, wing strokes up. Otherwise, downstroke motion is produced by longitudinal muscles via deforming the thorax roof in a longitudinal direction and raises the thorax roof upward, seen in Fig. 1-II. The indirect muscles of Dipteran insects are asynchronous muscles. In a word, the indirect muscles power wing movements by varying the elastic thorax's shape.

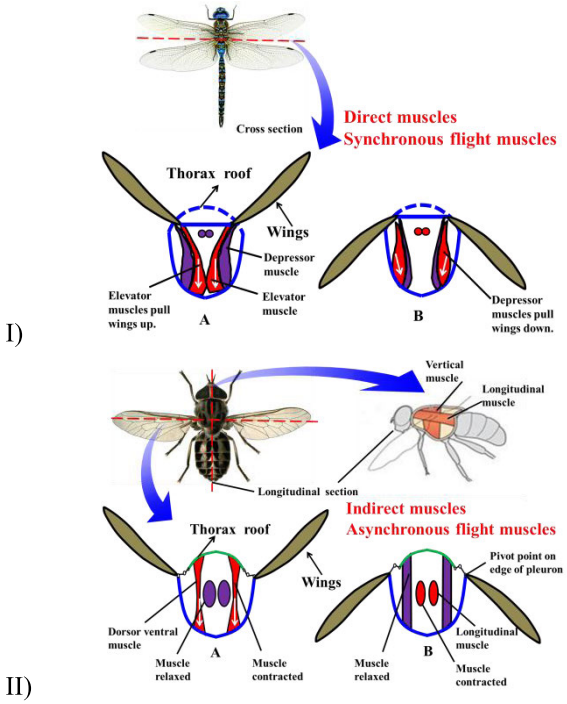

FIGURE 1. Diagrammatic cross-section of insect flight muscles. I) Thorax mechanisms of direct muscles: A) the wing is stroked up by contracting the elevator muscles; B) the wing is stroked down by shortening the depressor muscles. II) Thorax mechanisms of indirect muscles: A) the wings is stroked up by contracting the vertical muscles pulling the roof down B) by contracting the longitudinal muscles between anterior and posterior ends of a thorax, and elevating up the roof, the wing is stroked down, adapted from [14].

The flyers are capable of flapping at much higher frequencies with larger amplitudes for all the wings simultaneously, mainly thanks to the thorax acting as a resonant system. Meanwhile, active wing inversion of insects must originate at the wing base since their wings have no distal joints. Additionally, certain small insects like honeybees and fruit flies, the twist occur very close to the wing root when the wing approaches the end of the stroke, due to the aerodynamics and inertial loads. Also, the wing structure is very light, generally accounting for approximately 1% of the insect's weight [15], which rather differs from hummingbird wing construction.

Different insects adapted to different environment and needs, resulting in distinct flight mechanisms such as clap and fling in wasp [16], delayed stall and leading-edge vortex (LEV) in fruitfly and hawkmoth [17]. Therefore, certain insect-like FWMADs are developed based on these flight mechanisms, such as Micro Mechanical Fly [18], Harvard Robobee [19], KUBeetle [20], DelFly [21], TL-Flowerfly [22] and four wings aerial robotic flapper [23]. In addition, certain FWMADs mimicking the insect thorax mechanism were designed such as SU-8 [24], resonant thorax [25], a compliant thoracic mechanism [26]–[29]. Also, hummingbird-like FWMADs are developed based on the resonance principle [30].

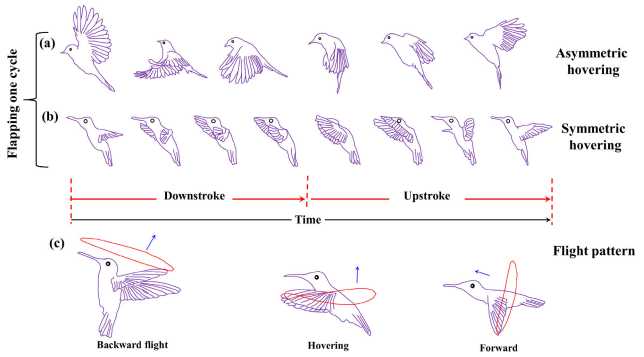

FIGURE 2. Flapping one cycle of an asymmetric hovering (a) and symmetric hovering (b), the flapping pattern of hummingbirds: eight-like pattern in hovering and oval pattern in other situations (c) adapted from [38].

B. MORPHOLOGY INTRODUCTION OF BIRD AND FLYER ROBOTICS INSPIRED BY THE BIRDS

In terms of birds, they have endoskeletons. The muscles attached to bones along the wing are applied for flight and maneuvering. Therefore, birds and flying insects have distinct flight mode. The birds with larger wings and weight spend the most time in forwarding flight with a low flapping frequency such as gliding, soaring. By contrast, hummingbirds can perform hovering flight with a high flapping frequency similar to the flight patterns of insect, thanks to the special morphological construction of hummingbird. For instance, the hummingbird's forearm bone and the upper arm are significantly shorter than that of a pigeon [31]. Although the birds' flight modes are different, the wing motion of all birds composes of upstroke and downstroke. The birds, excluding hummingbirds, flap their wings to balance the weight, and the circulations of strokes posed to generate the lift during the downstroke, whereas the drag is produced during the upstroke. Hummingbirds, however, generate aerodynamic lift in both upstroke and downstroke.

Hovering flight can be mostly discovered in flying insects and hummingbirds. Certain bats [32] and birds [33] are also able to fly in hovering, but they only use it in transitions (taking-off, landing and perching) since hovering requires more than twice the energy necessary for cruising [34] and more anaerobic metabolism.

In nature, there are two categories of hovering. Certain birds generate the most of lift during the downstroke when fully extending wings, and reduce drag by flexing their wings in the upstroke. Such kind of hovering is called asymmetric hovering [35] or avian stroke [36], shown in Fig. 2 (a). However, for the hummingbirds and insect, their wings remain fully extended throughout the wingbeat except for rotating and twisting at the end of each half stroke, which is called symmetric hovering or insect stroke, seen in Fig. 2 (b). In symmetric hovering condition, the body axis is inclined at a desirable angle and the wing presents an eight-like pattern in a vertical plane when hovering and an oval pattern is employed in most situations in forward and backward flight [37], [38], shown in Fig. 2 (c).

Due to the flight behaviors of hummingbirds, certain hummingbird-like FWMADs such as Nano-hummingbird [39], Micro-hummingbird [40], [41] and Giant-hummingbird [42], [43] were developed. However, there are still great challenges when designing FWMADs such as weight distribution of different components, energy-costing, wing design and tail's function. Therefore, the study of hummingbirds' morphologies is quite necessary and useful. This will not only help to understand the muscle kinematics in flight, skeleton structure and their aerodynamic mechanism, but also benefit from inspired FWMADs' development.

In this paper, a review of the morphology of the hummingbird in hovering flight is studied including muscle, construction of skeleton, aerodynamic in hovering, wing performance and tail performance. The comparison of motor mass and muscles mass of hummingbird are studied. The weight distributions of main components of FWMADs are also given. The designed wing inspired by the hummingbirds is presented based on scaling law. The wing efficiency is verified by a flight test. To explore the function of the tail, the inspired tail is introduced simply.

II. MUSCLE OF HUMMINGBIRD

The hummingbird's flight pattern is unique and insect-like, and they can easily hover, manoeuvre and even fly backwards. One reason is that they have a special physiological structure of muscles applied to control or modulate wing and body posture when flying. Another is that hummingbirds' aerodynamics allows for lift production in each half of stroke and achieves the characterized flight pattern by high wingbeat frequency, small muscle strains, and a highly supinated wing orientation during each end of strokes [44].

A hummingbird has massive muscles, shown in Fig. 3. However, the wing is mainly moved by a pair of powerful muscles: the pectoralis major (''depressor'' muscle or breast muscle) powers the downstroke and supracoracoideus muscles (''elevator'' muscles) are responsible for upstroke [45]. The breast muscle originates from the sternum like the breastbone and attaches near the bottom of the humerus (the upper arm bone), whereas the supracoracoideus muscle connects between the keel of the sternum and the top humerus. The wings flap down when the pectoralis major contracts, and flap up when supracoracoideus muscle shortens, shown in Fig. 4. The depressor is twice as heavy as the elevator, corresponding to the uneven lift production between downstroke and upstroke. The hummingbird muscles compose up to 30% of the body weight [37]. The pectoralis and supracoracoideus muscles are clearly shown in Fig. 3. Muscles activity of hummingbirds in hovering is shaded when flapping in the downstroke. The pectoralis is shown in Fig. 3 (A), whereas supracoracoideus muscles are displayed in Fig. 3 (B) and the pectoralis muscle is removed.

Birds separately operate muscles of pectoralis and supracoracoideus to flap downstroke and upstroke. The size of supracoracoideus in most of the birds is $1/5^{th}$ that of the pectoralis, which results in upstroke limitation aerodynamically.

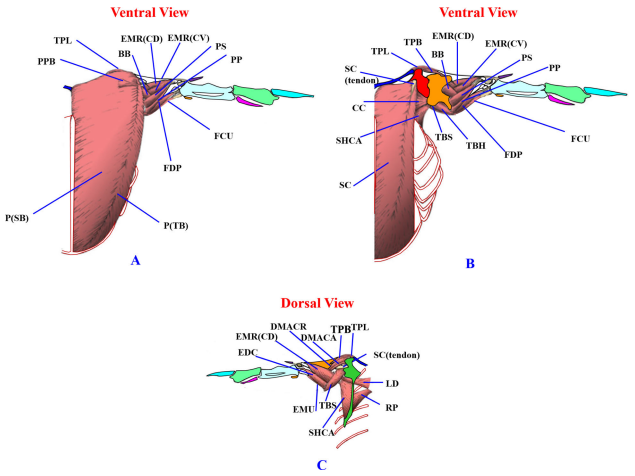

FIGURE 3. An illustration of the musculoskeletal anatomy hummingbirds, (A) the pectoralis muscle from ventral view, (B) the supracoracoideus muscle from ventral view, C) superficial muscles from dorsal view.BB, Biceps Brachii; CC, Coracobrachialis Caudalis; DMACA, Deltoideus Major Caudalis; DMACR, Deltoideus Major Cranialis; EDC, Extensor DigitorumCommunis; EMR (CD), Extensor Metacarpi Radialis (Caput Dorsale); EMR (CV), Extensor Metacarpi Radialis (Caput Ventrale); EMU, Extensor Metacarpi Ulnaris; FCU, Flexor Carpi Ulnaris; FDP, Flexor DigitorumProfundus; LD, Latissimus Dorsi (Pars Caudalis); P (SB), Pectoralis Major (Sternobrachialis); P (TB), Pectoralis Major (Thoracobrachialis); PP, Pronator Profundus; PPB, Pectoralis Pars Propatagialis Brevis; PS, Pronator Superficialis; RP, RhomboideusProfundus; SC, Supracoracoideus; SHCA, ScapulohumeralisCaudalis; TBH, Triceps BrachiiHumerotriceps; TBS, Triceps BrachiiScapulohumeralis; TPB, Tensor Propatagialis Pars Brevis; TPL, Tensor Propatagialis Pars Longa, adapted from [46].

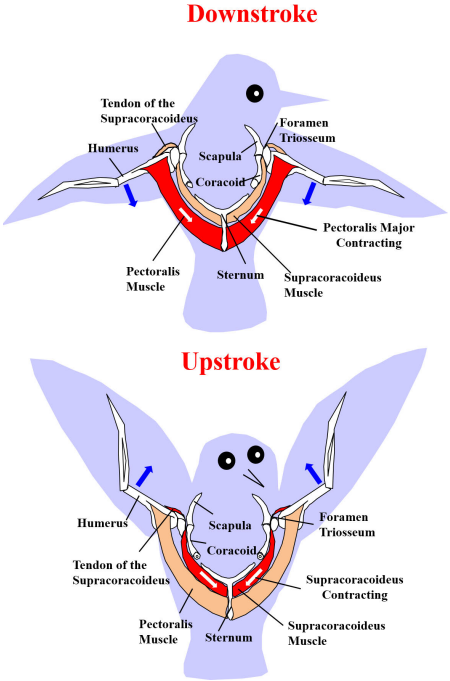

FIGURE 4. A schematic diagram of wing flapping for hummingbirds.

However, the flight muscle construction of hummingbird differs and they have almost the same size as pectoralis and supracoracoideus. The extreme proportion of two types of muscles is applied to complete the lift force generation in each half of stroke [46]. The reason that hummingbird is capable of flapping with high wingbeat frequencies and high aerobic power is mainly due to these large flight muscles widely include fast oxidative-glycolytic fibers as well as giant mitochondria, nearly occupying half of the total volume. Besides, the hummingbird is the highest mass-specific metabolic rates flyers, which means that hummingbird could switch fuels since high rates of sugar and fatty acid oxidation can satisfy high requirements of adenosine-triphosphate (ATP). For instance, the small hummingbirds have the highest known mass-specific metabolism for a vertebrate of around 40 ml oxygen per gram per hour (falling at rest to about 3 ml oxygen per gram per hour) when hovering [1]. Meanwhile, their flight muscles comprise 25-30% of their total body weight, a higher proportion than that of any other birds, and a higher density of mitochondria in flight muscles is 30% in hummingbirds, 40% in flies. Therefore, such special construction and contraction of flight muscle in hummingbirds contribute to a distinctive behavioral pattern. So to speak, the muscle composition ensures high wing beat frequency and required stroke amplitudes.

By studying the hummingbirds hovering flight, it is discovered that hummingbird always chooses two patterns to stay hovering, which are varying the wing-beat frequency and changing wing-motion stroke amplitude according to the density of surrounding air flow and additional mass of body [45]. However, due to physiological limitations of muscles, the stretching frequency and distances of muscles are inconsistent. Namely, the hummingbirds via the pectoralis and supracoracoideus muscles stretching cannot accomplish both in a high wing-beat frequency and larger wing-motion amplitude, which is paradoxical in physiological limitations. Therefore, there must be an optimal coupling value of each frequency and amplitude for hummingbirds when flapping [45].

A. MOTORS MASS VERSUS MUSCLE MASS OF HUMMINGBIRD

As we known, birds use flight muscle to drive their wings. However, as for the artificial birds, the DC motors are generally used to drive flapping mechanisms. The DC motor is selected for the three main reasons: 1) relatively wide choice of DC motors; 2) DC motor can be directly powered by the batteries; and 3) the motors have sufficient power to lift robots. However, the challenging is to choose an efficient motor, namely, the less weight the more sufficient power. To search inspiration in nature, the load-lifting capability between natural hummingbirds and hummingbird-like robots is compared, and the hummingbird flight muscles (defined as the summed mass of the pectoralis major and the supracoracoideus) and total lifted mass are survived in Appendix Table 4. In this table, the percentage of muscle over body mass and total lifted mass against body mass are also summarized. Furthermore, to analyze the load-lifting capability between the natural hummingbird and hummingbird-like robots, the hummingbird-like robots are also presented

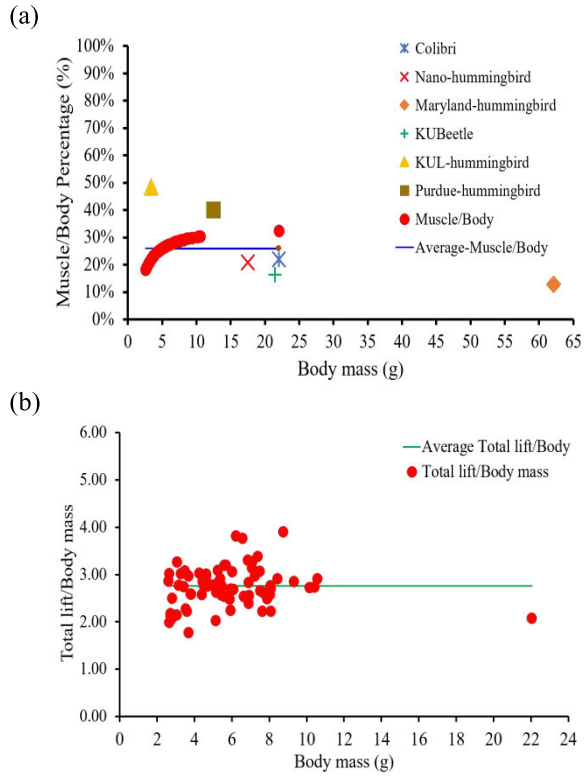

FIGURE 5. **(a) The comparison of hummingbirds and the hummingbird-like FWMADs of muscle mass over body mass and motor mass over FWMAD's body mass. (b) Total lifted mass over body mass of hummingbirds.**

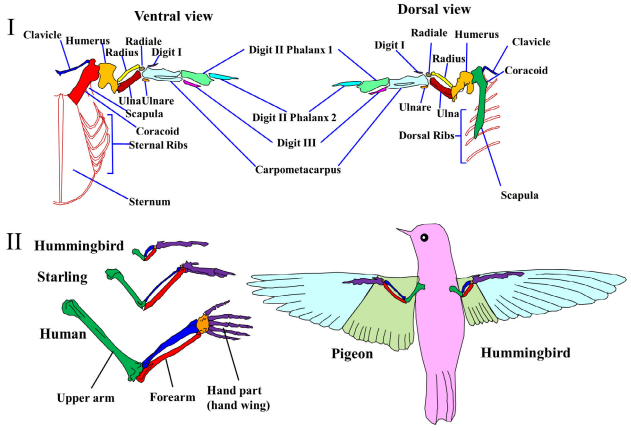

FIGURE 6. **(I) The skeleton of hummingbirds from ventral view (left) and dorsal view (right), (II) Wing morphology: size of forelimb bones with starling and human arm (left) and handwing size comparison of between hummingbirds and pigeon (right, handwing in light cyan).**

in Fig. 6, including weight distribution of main components. Some comparisons are presented graphically in Fig. 5. including both natural and man-made flyers.

From Fig. 5 (a), we can clearly see that the muscle's weight is about 20% ∼ 30% of body weight, 26% on average. Interestingly, the motor weight distributions are in the scope for the successful hovering flight man-made flyers (Colibri, Nano -hummingbird, Maryland-hummingbird and KUBeetle), even lower than that of average of the natural hummingbird like Maryland-hummingbird. This means that the higher efficiency motor is selected. However, the motor selections of KUL-hummingbird and Purdue-hummingbird seem not scientific, due to the high percentage of motor weight distribution. That is, designing other components will be constrained considering the vehicle's weight and lift generated by wings (A reasonable weight distribution of components may be important for designing a successful FWMAD). Surprisingly, the natural hummingbirds have a comparable load-lifting capability, which can generate lift about three times of their weights on average, seen in Fig. 5 (b).

III. THE SKELETON STRUCTURE OF HUMMINGBIRDS

Hummingbirds flap their wings in similar arcs and a high wingbeat frequency with large amplitude then achieve remarkable agility in flight. They must convert small muscle strains into large amplitude wing motions, or probably require changing the wing skeleton and flight stroke. Hummingbird's wing has a massive of skeletons shown in Fig. 6-I, but it can be simply considered that there are three parts (upper arm, forearm, and handwing, shown in Fig. 6-II (left)). By comparing the morphology of wing in hummingbirds and pigeons, the upper arm and forearm bones are much shorter than pigeons (the pigeon wing scaled to the hummingbird wing length) shown in Fig. 6-II (right), whereas the "hand" part of a wing, called hand wing, is relatively larger: over 75% handwing of entire wing area in hummingbirds to about 50% handwing in most of the birds [31]. Obviously, the most probable causes for these differences are the high wing-beat frequency, large stroke amplitude of hummingbird's flight, peculiar physiological structure and supracoracoideus muscles of hummingbirds. The shorter joint bones of elbows can be swift enough to enable hummingbirds to apply the high wing-beat frequency and large stroke amplitude flight pattern in a small muscle's strains dynamics. Compared with pigeons (scaled to hummingbird), the longer wing hand ossature (brown, manus) is applied to achieve extreme agile wing rotation [48], [49]. Besides, normal birds articulate their wings from shoulder, elbow, and wrist, whereas all the motion in hummingbirds only comes from the very mobile shoulder. Therefore, the wing rigidity is similar to that of insects and possesses similar flight characteristics. Hummingbirds can hover for a long period since they use symmetric hovering, also called insect stroke. Meanwhile, the hummingbird's wings are fully extended during downstroke to generate most of the lift force (about 70% of total lift), whereas approximately 25%-33% of the total lift is produced in upstroke as well as the drag is reduced by flexing wings in the upstroke. Rotating and twisting wings are placed at the end of each half stroke. In addition, it is interestingly discovered hummingbird wings are slimmer than that of pigeons, shown in Fig. 6. The details of wing morphologies will be discussed in the following section.

Recent studies revealed that most of the wing inversion is produced by supination of the forearm, namely, inverting

TABLE 1. The weight distributions of different components of hummingbird-like robots.

Species	Mass(g)	Motor (g) (PCT %)		Flapping mechanism (g) (PCT %)		Frame (g) (PCT %)		Wings (g) (PCT %)	
Colibri [51]	22.02	4.85	(22.00%)	2.91	(13.22%)	3.07	(13.94%)	0.48	(2.18 %)
Nano-hummingbird [39]	17.5	3.65	(21.00%)	2.47	(14.00%)	2.5	(14.00%)	0.26	(1.00%)
Maryland-hummingbird [42]	62.1	8	(12.90%)	8.7	(14.00%)	9.5	(15.30%)	1.7	(2.74%)
KUBeetle* [20]	21.44	3.5	(16.30%)	2.8	(13.10%)	1	(4.66%)	0.4	(1.87%)
KUL-hummingbird [40]	3.39	1.64	(48.37%)	1.08	(31.86%)		-	0.048	(1.42%)
Purdue-hummingbird [41]	12.5	5	(40.00%)	1	(8.00%)		-	0.1	(0.8%)

*The KUBeetle inspired by beetles, its size is closed to the hummingbird, so it is added for comparison.

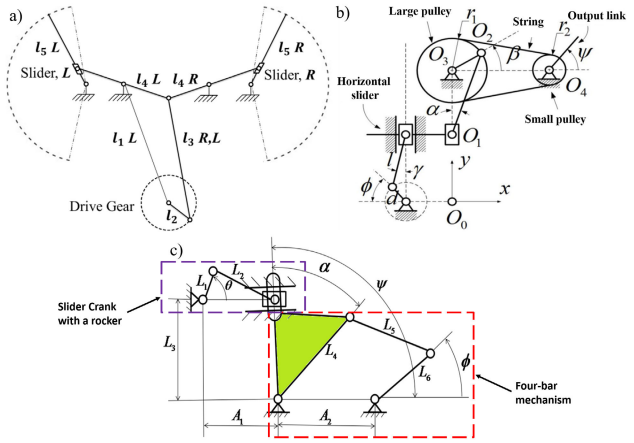

FIGURE 7. The flapping mechanism of three existing successful hovering flapping wing MAV: a) Maryland-hummingbird, b) KUBeetle, c) Colibri.

the bones (and feathers) of handwing [50]. The hummingbirds through moving the joints and rotating the three axes (spherical rotation, long-axis rotation, and polar rotation) are to achieve the wing flapping motion and wing rotation. By applying this approach, hummingbirds are able to flap the wings in a path to generate the required aerodynamic forces and to balance the weight in the unique flight patterns [50].

In hummingbirds, they drive muscles and bones to flap their wings. However, in order to generate flapping motion, many flapping mechanisms of FWMADs are developed and designed based on the different mechanisms such as dual serial four-bar linkage [39] and stroke-cam flapping mechanism [40]. The comparison study on flapping mechanisms of three hovering FWMADs is presented in [52]. This paper presented that no perfection design (uncertainty factors) on flapping mechanism may be compensated through an active control to make them stable flying. The flapping mechanism of three existing flapping wing MAVs are presented in Fig. 7. The flapping mechanism of Colibri as an example is discussed in this paper. There are two mechanism stages in the flapping mechanism: 1) slider crank with a rocker produce oscillation motion 2) a four-bar mechanism is for motion amplification. Angle θ is output angle from crank. Flapping amplitude ϕ, output angle of output link, can be obtained through following kinematics analysis. Also, compliant transmission mechanisms of FWMAD are summarized and reviewed as well in [14], [53]. In addition, the effects of elastic hinges flapping-wing compliant transmission mechanism is studied [54]. As for the flapping mechanism of Maryland-hummingbird, it is a novel and interesting flapping mechanism, which the five-bar linkage is applied in this robot. In this flapping mechanism, the four-bar linkage is firstly used to launch flapping motion driven by DC motor, and the fifth bar is then added to amplify the motion to the desired flapping amplitude. And as for the flapping mechanism of KUBeetle, two mechanisms are connected by the link bar and fix on the big pulley mechanism to transform flapping motion. In order to improve the flapping amplitude, the belt pulley mechanism is applied to amplify the flapping amplitude, then to reach desired angle.

In this paper, the flapping mechanism weight distributions of hummingbird-like robots are organized in Table 1. From this table, we can see that the weights of flapping mechanisms for successful hovering hummingbird-like robots are between in 13%∼ 14%. (At present, Colibri, Nano-hummingbird, Maryland-hummingbird and KUBeetle are successful hovering flight.)

IV. AERODYNAMICS OF HUMMINGBIRDS

Although hummingbirds and insects have evolved for sustaining hovering flight, the distinct phylogenies resulted in their different aerodynamic styles. In modern times, the kinematics of hovering hummingbirds was firstly studied in 1939 [55] and an aerodynamic model of hummingbird flight was developed in 1972 [56]. It is observed that the hummingbirds' flight feature is no dissimilar to insect flight, although hummingbirds operated at higher Reynolds number than that of insect. Therefore, it is hypothesized that similar kinematics and aerodynamic mechanisms are used in hummingbirds and insects when hovering [57]. In recent years, a number of studies on the kinematics, aerodynamics and flight dynamics of hummingbird are done, which reveals that how the hummingbird achieves its aerobatic feats [45], [58], [59].

Hummingbirds are capable of flying in hovering with fully extended wing during the entire wingbeat, which is related to the short humeral bones, long distal wing elements. However, by studying the wake of hummingbird wings, it was found that hovering in hummingbirds approaches that of insects, but remains distinct [60]. Hummingbirds produce pseudo-symmetrical wingbeat cycle in hovering, whereas insects exhibit an elegant aerodynamic symmetry. By studying Rufous hummingbirds hovering, 75% of the weight support is produced in the period of the downstroke, and only

25% during the upstroke [61]. Similarly, it is found that 66% of weight support in Anna's hummingbirds is generated during the downstroke in Wolf's study [62]. And the further study reveals that the far-failed wake of the hummingbird is remarkably similar to that produced by the hawkmoths [63]. Then the asymmetry is also presented partly due to inversion of the cambered wings during the upstroke. It means that such asymmetry was at least in part due to the positive camber of the hummingbird wings, which results in incomplete reversal during the upstroke. By contrast, the aerodynamic [64] and inertial forces [65] contributed by elastic qualities of insects wings allow their wings to reverse their camber fully, therefore, high lift coefficients can be created during both half-strokes [66]. On top of that, the ability producing the symmetrical wingbeat cycle for hovering hummingbird is strongly limited due to the fundamental musculoskeletal and the properties of platform materials, although strong similarities are present in the wing kinematics of hummingbirds consisting with certain insects such as hawkmoth and manducasexta.

Compared with insects' flight, the understanding of hummingbirds aerodynamics remains limited due to the highly complex morphology of vertebrate wings and the air flow related to their flight at low Reynolds numbers. However, certain aerodynamic mechanisms have been studied and understand improving lift across both insects and hummingbirds like a leading-edge vortex (LEV) which is a convergent solution to prevent the stall. For a flapping wing, the LEV remains stably attached as was first presented in paper [67] and confirmed by [68]. By the wake study of hummingbird wings, it is found that LEVs may dominate at low Reynolds numbers during the downstroke. However, LEVs is exploited as a key mechanism typical of insect hovering [68]. The attached LEV contributes to sustaining the high lift generation. Similar LEVs are also produced when hummingbird wings are modelled as flat plates [69]. And it is observed that a wide range of flyers or biological wings applies LEVs to control their flight [70]. By studying of robotic insects, it is found that such aerodynamic mechanism might improve lift by up to 45% in hovering fruit flies [68] and support up to two-thirds of the lift during the downstroke in hovering hawkmoths [63], [70], [71]. Up to 40% of lift is enhanced by the LEV in slow-flying bats [32]. For hummingbirds, it can occur up to 26% of the total lift in hovering [72] and about 50% of the lift in some forward flying birds [73].

Hummingbirds flap one cycle including downstroke and upstroke. Generally, the hummingbird wing rapidly decelerates at the end of upstroke, and re-accelerates at the beginning of the downstroke when rotating, further to say; the wings may pitch during translation to further enhance lift production. The path of the wingtip is more or less equal for both half strokes. By the wake study for hovering Rufous hummingbird in steady position [61], it is observed that there was sufficient circulation in the tip vortices and adequate separation between vortex cores. Wake structures consist of LEVs produced during the downstroke. The two cores of vortices, both rotating in the same direction, were shed in quick succession during the transition from downstroke to upstroke.

The key of using LEVs as lift mechanisms is that they are stable enough to remain attached to the wing during translation, rather than to be shed into the wake, as the lift will be lost when stalling. Birch and Lehmann's study reveals that the persistent LEVs are possibly made by stable flows at low Reynolds number [74], and such mechanism may be only available to small fliers [75], [76]. Certainly, some insects use wing rotation to produce lift when wing turning-around [68], that is to say, the wing rotation contributes to the high lift generation during stoke reversals of some wing kinematics, however, they also use the delayed stall mechanism to sustain the high lift generation during the stoke. And the circulation of the LEVs shed at the end of half-cycle can be re-captured in the subsequent reversing half cycle. Currently, by a theoretical and experimental study of aerodynamics, it is observed that a stable and attached LEV around hummingbird wings is primarily airflow when hovering, which is not dissimilar kinematics of insects. And the LEV is shed when translation ceases at the end of the downstroke, which results in lift decrease (except for next half-cycle translation re-started).

Warrick's study shows that LEVs are inconsistent and vary a lot from approximate 0.7 to 26% (16 % on average, for details to see [72]) of the total lift production when the hummingbird wing is strongly influenced by similar sharp-leading-edge aerodynamics [61], [72]. In addition, LEVs are always generated within 3mm of the dorsal surface of wings, showing no retrograde (trailing to leading edge) flow [72]. The bound circulations remain attached and persist, not shed as a vortex at the end of translation, and are augmented by the wing rotation between each half-cycle of the wing-translation. A near-continuous lift [72] can be generated by wing turning-around, which contributes to weight support, stability, and adjustment when hovering. At the same time, the chord length has been widely discussed with regard to the LEV formation and shedding [77].

Actually, the wake of a hummingbird in hovering mode is more complex. Different species of hummingbird may have distinct wakes when hovering. The study of Warrick *et al.* [61] suggests that 64% of weight support should be produced during downstroke at the slight differences in kinematics between the stroke phases. While, indeed, 66% (on average) of weight support in Anna's hummingbirds [62].

Regarding hovering Anna's hummingbirds, their wings generate individual ring structures in each stroke, and such wake consists of separate vortex loops for each wing. These vortex loops are shed at the end of the downstroke and move ventrally, whereas the shed loops move dorsally during the upstroke. In Wolf's study [62], it is discovered that 66% of weight support in hovering Anna's hummingbirds is generated during the downstroke. On top of that, the identified secondary vortex as a LEV is always shed at the end of the downstroke and varied considerably in strength. The 16% of weight support is produced on average by the secondary

vortex, which is similar to Rufous hummingbirds [61]. Similarly, 65% of support weight in the hovering hawkmoth is generated as well by the LEV [63]. Further study revealed that the strength of the vortex at the wing root is about 15% less than the circulation of the tip vortex but remains quite higher than that of slow-flying bats [62]. The root circulation in slow-flying bats was only 42% of that at the tip [32]. By wake measurement, it is indicated that a more evenly distributed vertical force of Anna's hummingbirds is produced between the wing strokes than that of hovering Rufous hummingbirds [62]. And the bilateral vortex was found in hovering Anna's hummingbirds with comparatively strong root vortices [62]. Similarly, a bilaterally symmetric wake with one vortex ring is also generated by each wing for bat [78]. Meanwhile, their wings are fully extended in hovering throughout the entire wingbeat cycle and generate lift during one cycle [57]. Although the bats produce a bilateral wake too, the span efficiency of the bat is lower than that of slow-flying flycatchers [32]. Therefore, it is guessed that the hummingbirds might also have lower span efficiency [32].

By contrast, from their visualization study, Pournazeri *et al.* [79] identified neither stop nor started vortices of the wake of hovering Anna's hummingbirds. They discovered separated stop vortices for the downstroke and started vortices for the upstroke, but also a combined start/stop vortex at the end of downstroke and the beginning of upstroke, in agreement with what has previously been identified for Rufous hummingbirds [61]. Transitions between stroke phases and wing rotations occur quickly, which can lead to a merge of individual vortex structures and result in complex wake configurations. Meanwhile, they found no bilateral vortex loops, which is different from Wolf's study. Nevertheless, although researchers could obtain different results for different species of hummingbirds when hovering, they have a common point that LEVs are playing essential roles for hovering hummingbirds.

To investigate the aerodynamics of hovering natural flyers, the full computational fluid dynamics (CFD) and the quasi-steady method have been used for the analysis of flapping wings. The full CFD models can provide more information about 3D flow pattern and force characteristics prediction, which is lack of the quasi-steady method. But the quasi-steady method is efficient tool for fast analysis as well as can revise the translation force, rotational force, and acceleration effect to address the unique features of flapping wings [68].

The study of aerodynamics on hummingbirds is quite important not only understanding on flight principle but also utilizing to control stability of flapping wing MAV. At present, many controllers are designed based on the aerodynamics of hummingbirds. Adaptive robust wing trajectory control was applied on flapping wing MAV [77]. A comparison of various aerodynamic models was studied on flapping flight stability in hovering [58]. Roshanbin A and Preumont A studied the yaw control torque generation in hovering hummingbird-like MAV [80]. And PD controller is applied as well in the hummingbird-like MAV [39], [42] [51].

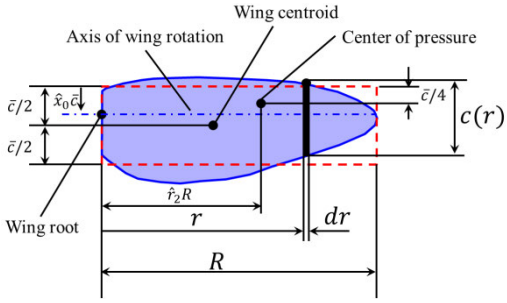

FIGURE 8. Wing geometry parameters with wing radius R, local radius r, chord length $c(r)$, mean chord length $\bar{c}$, $\hat{x}_0$ is the non-dimensional position of the rotational axis. $\hat{r}_2$ is the non-dimensional radius of the second moment of inertia.

V. MORPHOLOGY OF WINGS AND GEOMETRIC SIMILARITY

Hummingbird wings are relatively small, narrow and extremely thin at the leading edge. Thanks to the unique wing shape, the sharp leading edge creates a leading edge flow that produces greater lift. Recent analytical studies have shown that the wing planform of hummingbirds which has more area towards the root (i.e. wing area centroid more towards the root) is very efficient in lift generation production. There are some factors to describe the wing shape such as a lumped parameter, aspect ratio and wing loading. Wing loading and aspect ratio are widely applied to quantify the size and shape of aircraft engineering and in studies of animal flight. In certain researches, relative wing loading (RWL) is utilized to estimate the aerodynamic performance [35]. In this paper, a flat and rigid wing in arbitrary form is hypothesized. The wing geometry parameters are presented in Fig. 8. In this section, wing morphology and geometric similarity are to be studied and discussed.

If birds are hypothesized to be a geometric similarity, then weight and lift can be expressed a characteristic length l during the steady-state flight. The entire wing surface A including two wings in vertebrate flyers with projected body area and volume V varies with characteristic length, that is,A $\sim l^2$, V$\sim l^3$. In hovering or steady forward flight, it is reasonable to assume that the weight is proportional to lift force $\bar{F}_L$.

$$W \sim \bar{F}_L \sim \frac{1}{2} C_L \rho v_t^2 A \tag{1}$$

where, C_L is the lift coefficient, ρ is the density, v_t is the forward flight velocity.

$$W = mg \sim \bar{F}_L \sim V \sim l^3 \tag{2}$$

where , W is the weight, m is the mass of flyer, g is the gravitational acceleration.

Total surface can be written as [81]

$$A \sim l^2 \approx (m^{\frac{1}{3}})^2 \approx m^{\frac{2}{3}} \tag{3}$$

A. WING LOADING

Wing loading is an important parameter on the flight mechanism of flyers, which is defined as the weight of flyer divided

by the entire wing surface, and is expressed as follows:

$$p_w = mg \Big/ A \sim v_t^2 \sim l \sim m^{1/3} \tag{4}$$

Clearly, wing loading varies with size and is proportional to the third root of body mass as a result of inclining to be larger in larger animals and artificial flyers. Besides, it has an equivalent unit of pressure, so it also presents the pressure force over the wing. Importantly, it is proportional to the square root of the flight speed, which indicates that flyers with low wing loadings can fly at slow speed. By contrast, flyers with larger weight have larger wing loading and must fly fast. Manoeuvrability depends on wing loading because it relies on the minimum radius of turn which is proportional to body mass [82]. It means that manoeuvrability rises with wing loading decrease. Therefore, we could see that the aircrafts utilized in aerobatics has small wide wings with low wing loading.

B. ASPECT RATIO

The aspect ratio (AR) is a parameter of the wing performance of flyers and a measure of the shape of the wing, which significantly represents the wing geometric shape of flyers [83]–[86]. Importantly, it further impacts the aerodynamic efficiency. It is defined as the square of the wing span over the surface of the wing pair, which AR is presented as follows:

$$AR = (2R)^2 \Big/ 2S = 2R^2 \Big/ S \sim l^2 \Big/ l^2 \sim m^0 \tag{5}$$

It can be rewritten as

$$AR = 2R^2 \Big/ S \approx 2R^2/(mg/2p_w) \approx (4R^2/mg)p_w \tag{6}$$

From Equation (4), it shows that aspect ratio does not vary with body mass. However, according to the following study, the aspect ratio slightly varying with the size is discovered, which is different from the study presented in paper [87].

In general, flyers with small AR have high agility and maneuverability, whereas the higher AR the wing has, the better energy efficiency [88], [89], which in turns leads to higher lift production. Also, a high AR wing contributes to a low induced drag which benefits from gliding and slow flapping flight. Namely, glide ratio (the lift-to-drag ratio) rises with aspect ratio increasing [87]. For instance, the aspect ratio of hummingbirds (approximately 6.5 $\sim$ 9.5) is less than that of albatross (approximately 15), so albatrosses fly in gliding most of the time, while hummingbirds are capable of hovering. Besides, increasing the aspect ratio will enhance the lift coefficient in a certain ranges when the attack angle is constant, so aerodynamic performance can be improved by increasing aspect ratio in a certain ranges, the similar states were presented, see in paper [13], [90], [92], [93]. Higher aspect ratio makes wing longer and thinner. However, long wings not only induce drag due to wingtip vortices but also are more vulnerable to break the wing, and might be negative to take-off from the ground. Thus, the different combinations of wing loading and aspect ratio allow a natural flyer to adopt particular flight pattern and foraging strategies [94]. And the concept of $p_w - AR$ ratio is introduced in paper [81], which is $\frac{p_w}{AR} = \frac{mg/A}{2R^2/S} \approx \frac{mg}{2S} \cdot \frac{S}{2R^2} = \frac{mg}{4R^2}$ (N/m^2). $p_w - AR$ Ratio has the same physical unit of wing loading, so it may be used to evaluate the wing performances as performance index, detail see in paper [81].

C. WING LUMPED PARAMETER K

Lumped parameter (k) is also essential for wing design and reveals the relation between flapping wing frequency and body morphology (i.e., total wing surface and body mass). Corben [95] exhibited the relationship between flapping frequency, entire wing surface and body weight based on the non-dimensional analysis, which is expressed as

$$f = \frac{k}{A}\sqrt{\frac{mg}{\rho}} = \frac{g}{\rho}\frac{k}{A}\sqrt{m} = 2.86\frac{k}{A}\sqrt{m} \tag{7}$$

$$k = \frac{fA}{2.86\sqrt{m}} \sim \frac{m^{-\frac{1}{6}}m^{\frac{2}{3}}}{m^{-\frac{1}{2}}} = m^0 \tag{8}$$

The cycle average lift force of a pair of flapping wings can be expressed as $\bar{F}_L = \frac{1}{2}\rho\bar{C}_L AR(S\emptyset f)^2$ then mean lift coefficient can be expressed as $\bar{C}_L = \frac{2\bar{F}_L}{\rho AR(S\phi f)^2}$ [78], [96] and the combination of Equation (7), the hypothesis of $\bar{F}_L = mg$, relationship of wing lumped parameter with $\bar{C}_L$ and AR can be presented as

$$k = \frac{2\sqrt{2}}{\bar{C}_L\emptyset\sqrt{AR}} = \frac{2\sqrt{s}}{\bar{C}_L\emptyset R} \tag{9}$$

The lumped parameter is also a dimensionless number. From Equation (8), we found that it is independent of body mass. The lumped parameter is inversely proportional to the average mean lift coefficient, which indicates that the larger lumped parameter it is, the less lift is produced at a constant angle attack. Besides, the larger lumped parameter is, the shorter and rounded wing is since the lumped parameter is also inversely proportional to the aspect ratio. Therefore, the lumped parameter can also be regarded as a measure of aerodynamic efficiency and be used to supervise wing design.

Hummingbird wings are highly variable in size, with wing length ranging from 35 to 152 mm among species [97]. And aspect ratio ranges are from approximately 6.5 to 9.5. Notably, certain modern flyers have a similar aspect ratio such as Boeings (737 and 747), and aerodynamic performance in advanced micro helicopter rotor is remarkably similar to that of hummingbirds [98]. The wing parameters of hummingbirds are summarized in Appendix Table 5 including mass, flapping frequency, wing surface, wing loading, aspect ratio, and lumped parameter. The wings of 12 different species hummingbirds are presented in [98] and it is clearly exhibited that the wings of hummingbirds are longer, thinner and slimmer relative to their sizes, which is also verified in Fig. 6.

D. SCALING LAW, RESULTS AND DISCUSSION

In this subsection, the scaling laws induced by regression analysis of species of hummingbirds are established based

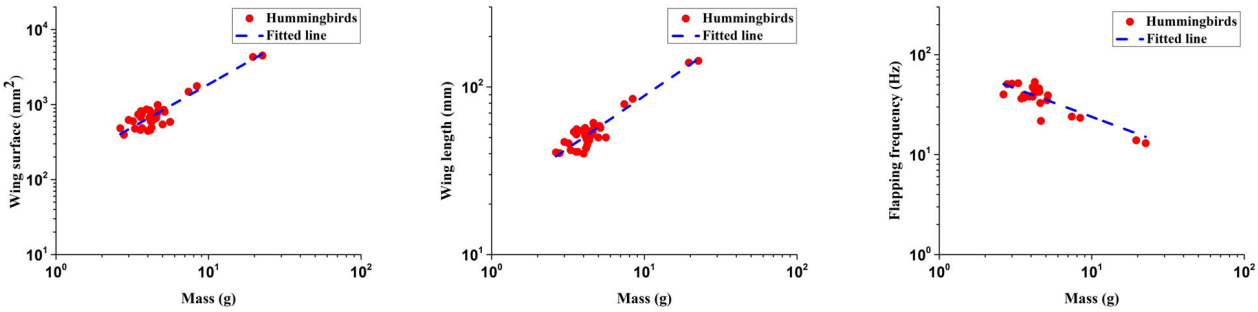

FIGURE 9. The relation of wing surface vs. mass (left), the fitted line corresponds to $S=133.42m^{1.15}$; wing length vs. mass (mid), $R=21.07m^{0.62}$; flapping frequency vs. mass (right), $f=88.25m^{-0.57}$.

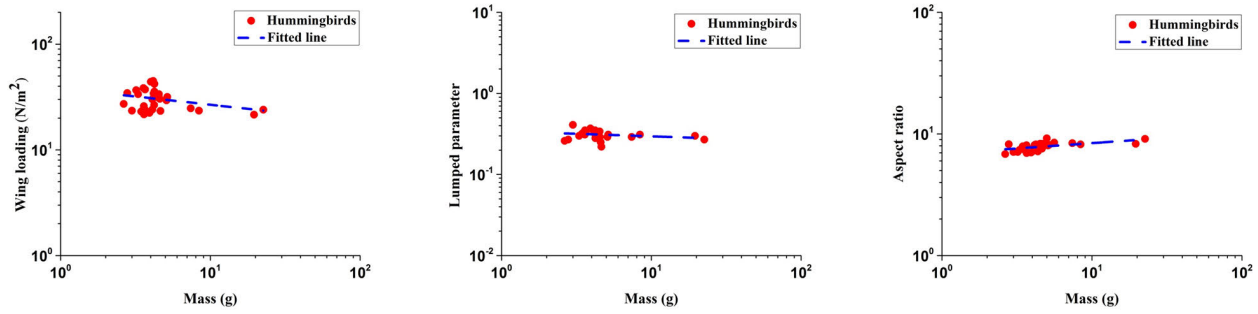

FIGURE 10. The relation of wing loading vs. mass (left), $p_w = 38.27m^{-0.16}$; lumped parameter vs. mass (mid), $k=0.34m^{-0.06}$; aspect ratio vs. mass (right) $AR=6.9m^{0.09}$.

on the concept of geometric similarity. The relation between weights and parameters of wing performance can be predicted and determined before being applied in designing the hummingbird-size FWMAD. In other words, this concept provides rules to design and compare flying objects within different sizes and weights through several orders of magnitude.

Summarized plots of the relationship among wing surface, flapping frequency and wing length against body mass are firstly presented. The fitting curve is provided in blue color. Fig. 9 exhibits that the figures are intensive with an excellent general tendency. Wing surface and wing length are proportional to body mass in a log-log domain, whereas the flapping frequency is inversely proportional to the body mass, shown in Fig. 9 (right). The fitted functions of wing surface and mass, wing length and mass, and flapping frequency and mass are given in the Fig. 9.

VI. SCALING LAW, RESULTS AND DISCUSSION

In this subsection, the scaling laws induced by regression analysis of species of hummingbirds are established based on the concept of geometric similarity. The relation between weights and parameters of wing performance can be predicted and determined before being applied in designing the hummingbird-size FWMAD. In other words, this concept provides rules to design and compare flying objects within different sizes and weights through several orders of magnitude.

Summarized plots of the relationship among wing surface, flapping frequency and wing length against body mass are firstly presented. The fitting curve is provided in blue color. Fig. 9 exhibits that the figures are intensive with an excellent general tendency. Wing surface and wing length are proportional to body mass in a log-log domain, whereas the flapping frequency is inversely proportional to the body mass, shown in Fig. 9 (right). The fitted functions of wing surface and mass, wing length and mass, and flapping frequency and mass are given in the Fig. 9.

The relation of wing loading, lumped parameter and aspect ratio with body mass are shown in Fig. 10. From this figure, we observe that the three relations do not follow the rules induced by geometrical similarity. The wing loading is inversely proportional to weight. The similar results are achieved in [105]. Actually, the wing loading generally rises with the size increase for natural flyers excluding hummingbirds. Regarding k and AR, both slightly vary with weight. Therefore, it is roughly considered that AR is independent of size, a similar result also stated in [105]. The fitted functions of wing loading and mass, lumped parameter and mass, and aspect ratio and mass are present in the Fig. 10. In this study, the statistical mean value of AR is presented, which is expressed as a mean value with standard deviation, $AR=7.86\pm0.56$ and the statistical mean value of the lumped parameter is about 0.31 ± 0.04.

At present, certain FWMADs inspired by hummingbird are developed, which is summarized in Table 2. Since the wing loading and aspect ratio are widely applied to quantify the size and shape in aircraft engineering and in studies of animal flight, the plot of aspect ratio and lumped parameters against

TABLE 2. Parameters of existing flapping-wing MAVs.

Species	m (g)	R (mm)	f (Hz)	S (mm^2)	p_w (N/m^2)	RWL	AR	∅(deg)	k
Colibri [51]	22.02	90	22	1816	52.43	19.04	8.9	180	0.21
Nano-Hummingbird[39]	17.5	68	27.5	1768	49.5	19.06	5.2	180	0.26
Maryland-Hummingbird[42]	62.1	140	20	9232	33.4	8.5	4.2	120	0.52
KUBeetle[20]	21.4	70	25-35	1750	50.7	22.02	5.6	190	0.3

* Since the Wing parameters of KUL- and Purdue- hummingbird are less, they are not analyzed comparably.

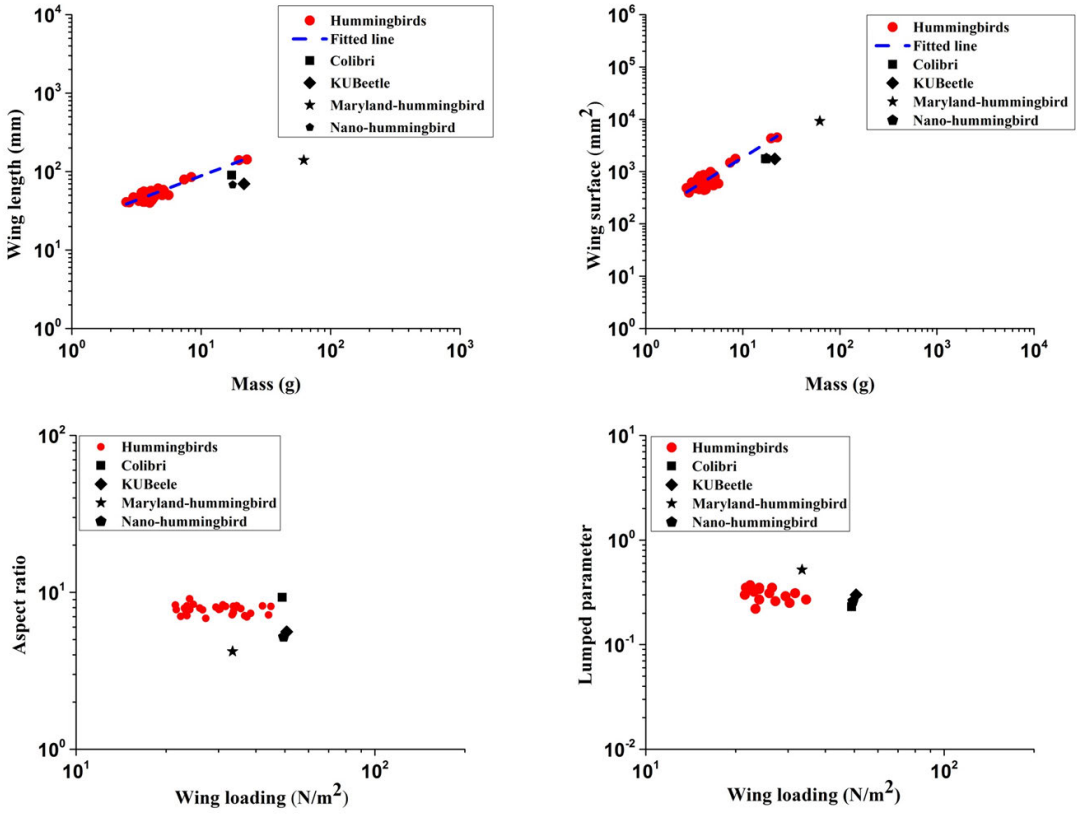

FIGURE 11. Wing performances of natural hummingbirds compared with the hummingbird-like FWMADs.

wing loading are given for comparing the wing performance of natural hummingbirds and hummingbird-like MADs. And wing length and surface as basic and useful parameters are also utilized for comparison. The compared figures are shown in Fig. 11. This figure displays that the data are intensive and existing FWMADs (except Maryland-hummingbird) are nearly in the range of species and are following these scale rules. The size of Maryland-hummingbird is actually in the scope of bats. Meanwhile, the KUBeetle inspired by beetles, its size is closed to the hummingbird, so it is added for comparison. In addition, the wings of Colibri (hummingbird-like MAV) are designed based on the above-studied scale laws, and the efficiency of wings is verified by flight experiment, shown in Fig. 12. In this figure, the flapping mechanism is shown in Fig. 12 a), which is composed of two stages 1) slider crank with a rocker 2) four-bar mechanism. The wings construction is given in Fig. 12 b) (Details of wing manufacture can be seen the study of Nan *et al.* [96]), the certain selected wings are presented in Fig. 12 c), and the integrated MAV with sail is given in in Fig. 12 e), and flying demonstration is shown in in Fig. 12 d). Additional details of wing designs based on different materials and methods are summarized in Appendix Table 6. Besides, Zhang did the similar jobs on wing design, optimization and system integration of robotic hummingbird [41].

VII. MORPHOLOGY OF TAILS

As we known, wing shape is remarkable essential since the wing shapes are directly related to flight modes. Also, the bird's tails play an important role in maintaining stability over a range of flight speeds and in generating lift and drag to help roll, pitch and yaw turning and slow flight. Bird's tails vary as much as their wings, or even more [106]. The tail shapes and morphology of birds are naturally selected by gender. The birds' tails have intricate and distinct shapes particular in sexually dimorphic species. Many birds have a long and elaborate tail as a sexual ornament since long and elaborate tails can enhance mating success for female

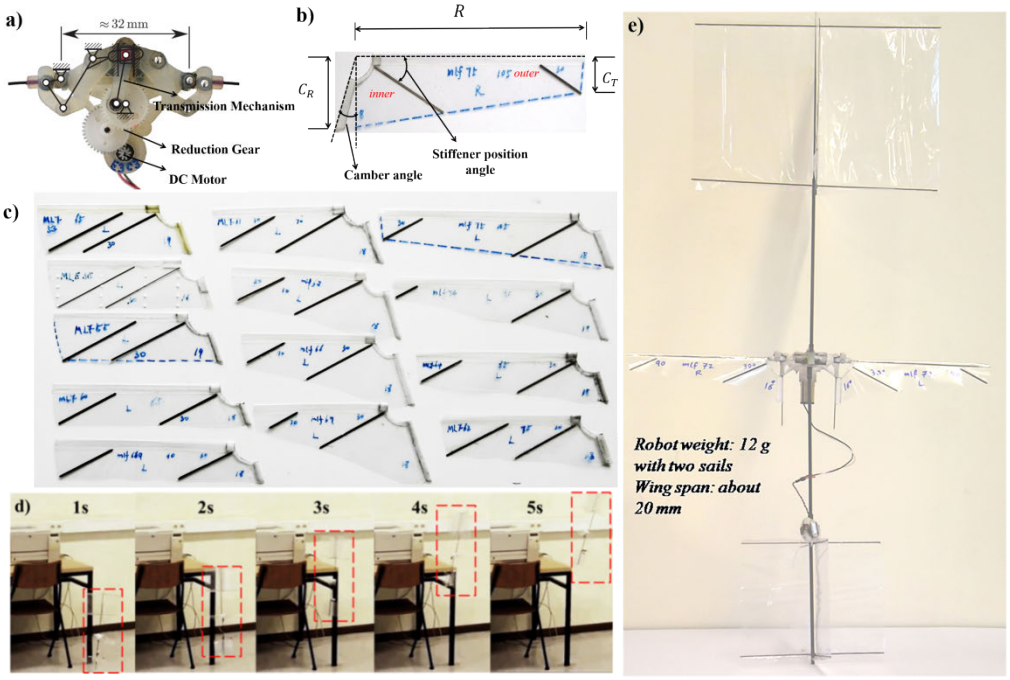

FIGURE 12. Flight demonstration with sail-like damper for passive stability [117]. a) Flapping mechanism, b) Wing geometry: C_T wing tip chord, C_R wing root chord, c) Certainly selected wings, d) Flight sequence, e) An assembled prototype with sail. The full video recording is available online: https://www.youtube.com/watch?v=VLmOt_ktLEw.

TABLE 3. The geometric parameters of tail.

	Spread angle β	Tail Surface S_t(mm^2)	AR_t	Span b_t (mm)
Tail-R_{67}	67	2863.5	2.08	77.2
Tail-R_{120}	120	5128.7	2.86	121.2
Tail-T_{120}	120	2123.1	2.86	121.2

R- Rounded tail, T- Triangular tail. R_{67} is the rounded tail with 67°, R_{120} is the rounded tail with 120°, and T_{120} is the triangular tail with 120°.

choice [107]. However, flight performance might be constraint such ornamental diversity [108].

Universally, different birds select different tail shape, but they have a common feature, namely, the tails play an aerodynamic role in flight [109]–[112], as the birds' tail directly affects stable flight, and they can use their tails to operate body turns [113]–[115]. Also, hummingbirds may use tail spreading to stabilize their posture [59], [116].

In this section, hummingbird tail morphology and tail design and manufacture will be introduced. The detail of tails will be studied in the future. All hummingbirds have five bilateral pairs of rectrices (the tail feathers are called rectrices) that individually vary in length and shape [108]. The number of rectrices is marked from medial R_1 to lateral R_5, seen in Fig. 13. From such figure, outer tail feathers are longer than the middle pair in the forked tail, and feathers increase in length from the central pair to the outer pair. That is, R_5 is the longest of rectrice, whereas R_1 is the shortest one. By contrast, as for graduated tails, R_1 is the longest and R_5 is the shortest rectrix. All rectrices in rounded tails are of almost the same length, feathers increase in length from the outer pair to the middle pair. The length of the longest rectrix is 20%

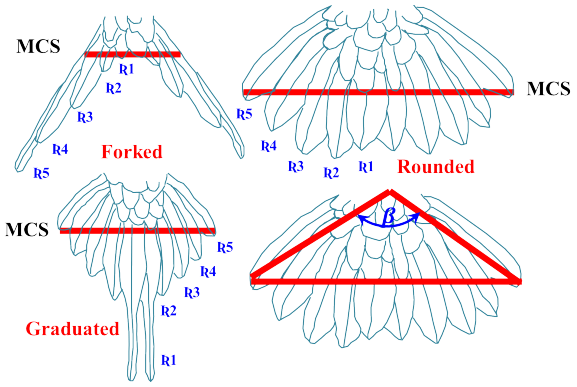

FIGURE 13. Tail shape and spread angle. R has represented the rectrix feather of the tail.

more than that of the shortest one. The maximum continuous span (MCS) is the widest distance of the unbroken surface area of a tail, from R_5 to R_5 on both lateral sides. The spread angle is the angle between the outermost rectrices presented by β, seen in Fig. 13. When this angle is above a critical value, the gap between individual tail feathers has appeared. By contrast, the edges of neighbouring tail feathers overlap

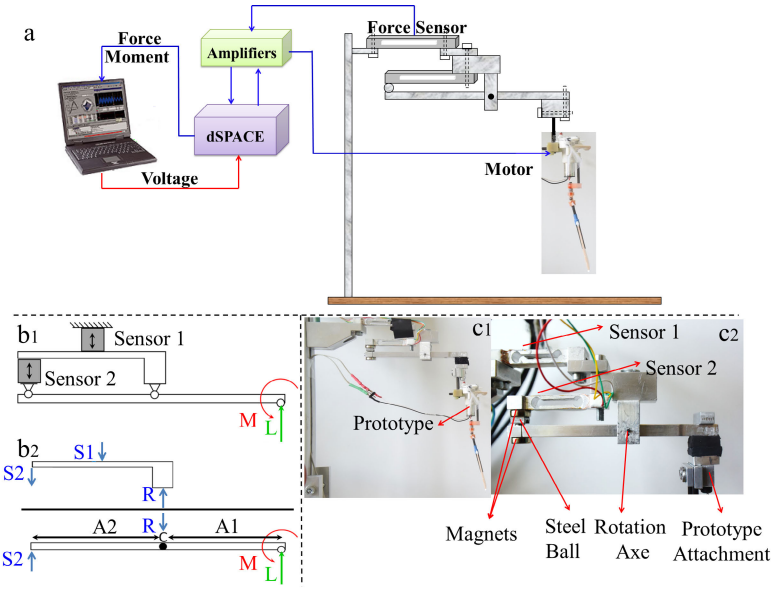

FIGURE 14. The experimental setup. Schematic diagram of the complete setup (a), the working principle with a free body diagram (b1+b2), the photos of the physical implementation (c1+c2).

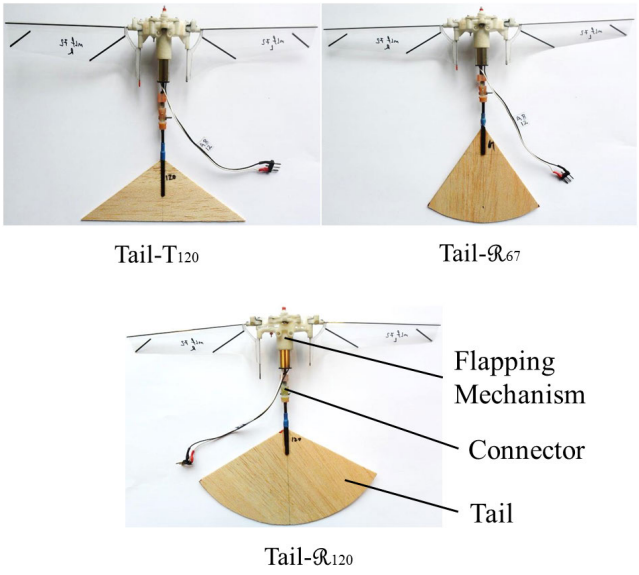

FIGURE 15. Assembled prototype with wing and tail [119].

when this angle is smaller than the critical angle. Therefore, the tail's surface (SA) [108] can be roughly approximated as

$$SA_{tail} = \frac{1}{2}\mathrm{R}_n^2\beta \tag{11}$$

where, R_n is the average length of the tail feather.

Fork ratio (FR) is an important parameter to shape the bird's tail, which is defined as defined as the R_5 length divided by the R_1 length, which is presented as

$$\mathrm{FR} = \mathrm{R}_5\mathrm{length}/\mathrm{R}_1\mathrm{length} \tag{12}$$

When fork ratio is higher than 2 (FR $>$ 2), the tail shape can be roughly defined as an elongated fork tail. The optimal fork ratio is FR $= 2$ at $\beta = 120^\circ$ [92], [106], but this spread angle is not general. After that, it is also explored that the optimal fork ratio is 1.2 when $\beta = 67^\circ$. When fork ratio is in the range of $1.2 < \mathrm{FR} < 2$, the tail shape can be regarded as a moderate fork. As for the rounded tail, the fork ratio is in $0.83 < \mathrm{FR} < 1.2$, whereas the graduated tail may be achieved at FR < 0.83.

Tail aspect ratio [118], similar wing aspect ratio, is a measure of the shape of the tail and impacts on the aerodynamic performance. It is defined as the square tail span divided by the tail surface, which is given by

$$AR_t = b_t^2/S_t \tag{13}$$

where, b_t is the tail span which can be calculated by $b_t = 2\mathrm{R}_5 sin\frac{\beta}{2}$ and S_t is the tail surface.

Combination of Equation (11) and (13), the tail aspect ratio can be rewritten as

$$AR_t = \frac{b_t^2}{S_t} = \frac{2b_t^2}{\mathrm{R}_n^2\beta} \tag{14}$$

To compare morphologies, the spread angle is hypothesized to be constant, whereas the spread angle actually varies with flight posture.

To investigate the tail's aerodynamic performance, a family of the tail was built [119] and an experimental setup consisting of a force balance, voltage amplifiers, and a digital signal processing system (DSP) was constructed [96]. Its overview is illustrated in Fig. 14. In Nan's study [119], the designed tail based on the mimicking hummingbird's tail is made of the balsa wood with 1 mm thickness. The tail with a maximum tail length of 70 mm is made. The designed-tails were handmade, as is shown in Fig. 15. In total, three kinds of tails were built and tested, and the parameters are presented in Table 3. Via studying the experiment, results show that tails

can be used to stabilize the posture of birds by generating a moment [119], which is similar to the presented result in [59], [106], so it can be applied to the FWMADs to balance the posture. This means that the posture of FWMAD can be performed via adjusting the position of the tail. In the previous study of twin-wing hovering FWMADs, however, the wing twist modulators [20], [39], [42], [43], [120] were universally applied to produce pitch and roll moment then achieved the stability of FWMADs. In addition, recent study of tail [117] is successfully used on passive stability of FWMADs.

VIII. CONCLUSION

In this paper, the insects and birds morphologies are firstly introduced, followed by the morphology study of hummingbird including the muscles, skeleton structure to investigate the hummingbird flying, in which the weight distribution of each component and flapping mechanisms are studied. The reasonable weight distribution of components is important to design a successful FWMAD. After that, the aerodynamic of hummingbirds is presented to interpret the reasons of hovering flight. Then, the scale laws and geometry similarity are explored and summarized before obtaining the relations between parameters of wing performance and weight. The wings are designed based on the scale laws and wing's efficiency is also proofed by flying test. Therefore, the studied scale laws in this paper may be reasonable and acceptable. Also, designed wings based on different materials and methods are summarized. Last, the morphology of tail is studied and designed tails are discussed. The results show that a tail may be employed in hovering stability of twin-wing FWMADs. Therefore, we believe that the current studies provide a simple but useful dataset and guideline for biologists and engineers who study the morphology of hummingbirds and future development of similar sized FWMADs.

Our future research will focus on further experimental research and the FWMAD's reliability design and improvement under uncertainties using artificial intelligence driven approaches [133], [134], [136]–[138], [140]–[144].

APPENDIX

TABLE 4. Body, muscle parameters of various hummingbird species adapted by [47].

Species	Body mass (g)	Muscle mass (g)	Total lifted mass (g)	Muscle/Body (%)	Total lift / body
Acestrura mulsant	3.527 (0.110)	0.796 (0.038)	8.047 (0.100)	23%	2.28
Adelomyia melanogenys	3.472 (0.114)	0.777 (0.039)	10.718 (0.355)	22%	3.09
Aglaeactis castelnaudii	7.500 (0.240)	2.159 (0.082)	19.926 (0.219)	29%	2.66
Aglaeactis cupripennis	7.064 (0.099)	2.009 (0.034)	22.221 (0.721)	28%	3.15
Aglaiocercus kingi	4.653 (0.379)	1.182 (0.130)	12.853 (1.487)	25%	2.76
Amazilia amabilis	4.234 (0.277)	1.038 (0.095)	12.858 (0.644)	25%	3.04
Amazilia decora	4.625 (0.112)	1.172 (0.038)	13.935 (0.934)	25%	3.01
Amazilia edward	4.419 (0.065)	1.102 (0.022)	12.624 (0.558)	25%	2.86
Amazilia saucerrottei	4.491 (0.518)	1.126 (0.178)	12.419 (2.558)	25%	2.77
Amazilia tzacatl	5.324 (0.088)	1.412 (0.030)	15.290 (0.548)	27%	2.87
Archilochus alexandri	3.034 (0.086)	0.627 (0.030)	6.534 (0.307)	21%	2.15
Archilochus colubris	3.670 (0.244)	0.845 (0.084)	6.517 (0.502)	23%	1.78
Boissonneaua matthewsii	7.876 (0.223)	2.287 (0.077)	19.651 (1.201)	29%	2.50
Campylopterus hemileucurus	10.406 (0.467)	3.155 (0.160)	28.504 (1.059)	30%	2.74
Campylopterus largipennis	8.723 (0.193)	2.578 (0.066)	34.071 (1.447)	30%	3.91
Chalcostigma ruficeps	3.808 (0.181)	0.892 (0.062)	9.864 (0.590)	23%	2.59
Chalcostigma stanleyi	6.000 (0.518)	1.644 (0.178)	18.362 (2.558)	27%	3.06
Chalybura urochrysia	6.886 (0.197)	1.948 (0.068)	19.524 (1.274)	28%	2.84
Chlorostilbon assimilis	2.739 (0.518)	0.525 (0.178)	5.650 (2.558)	19%	2.06
Chlorostilbon mellisugus	3.144 (0.165)	0.664 (0.057)	8.750 (0.717)	21%	2.78
Chrysuronia oenone	4.611 (0.102)	1.168 (0.035)	13.763 (0.671)	25%	2.98
Coeligena violifer	8.028 (0.208)	2.340 (0.071)	20.729 (0.749)	29%	2.58
Colibri coruscans	7.681 (0.174)	2.221 (0.060)	20.121 (0.481)	29%	2.62
Colibri thalassinus	5.578 (0.338)	1.499 (0.116)	17.871 (1.680)	27%	3.20

TABLE 4. ***(Continued.)*** **Body, muscle parameters of various hummingbird species adapted by [47].**

Doryfera ludovicae	5.462 (0.084)	1.460 (0.029)	15.091 (0.885)	27%	2.76
Elvira chionura	3.260 (0.090)	0.704 (0.031)	9.855 (0.480)	22%	3.02
Eriocnemis sapphiropygia	6.907 (0.142)	1.955 (0.049)	17.690 (1.043)	28%	2.56
Eugenes fulgens	7.487 (0.089)	2.154 (0.030)	23.020 (0.692)	29%	3.07
Eugenes fulgens	9.306 (0.309)	2.778 (0.106)	26.561 (1.650)	30%	2.85
Eupherusa eximia	4.495 (0.118)	1.128 (0.040)	12.760 (0.628)	25%	2.84
Eutoxeres aquila	10.139 (0.089)	3.064 (0.030)	27.709 (0.089)	30%	2.73
Eutoxeres condamini	10.562 (0.181)	3.209 (0.062)	30.787 (2.787)	30%	2.91
Florisuga mellivora	6.845 (0.226)	1.934 (0.078)	22.655 (1.172)	28%	3.31
Glaucis aenea	5.913 (0.361)	1.614 (0.124)	13.284 (0.570)	27%	2.25
Glaucis hirsuta	7.219 (0.210)	2.062 (0.072)	21.472 (1.068)	29%	2.97
Haplophaedia assimilis	5.120 (0.518)	1.342 (0.178)	10.430 (2.558)	26%	2.04
Heliangelus amethysticollis	5.882 (0.183)	1.604 (0.063)	14.635 (0.446)	27%	2.49
Heliodoxa aurescens	6.200 (0.110)	1.713 (0.038)	23.669 (0.551)	28%	3.82
Heliodoxa branickii	6.565 (0.115)	1.838 (0.039)	24.756 (3.729)	28%	3.77
Heliodoxa jacula	8.067 (0.234)	2.353 (0.080)	21.853 (1.455)	29%	2.71
Heliodoxa leadbeateri	7.372 (0.092)	2.114 (0.032)	25.004 (1.327)	29%	3.39
Heliomaster longirostris	7.611 (0.335)	2.197 (0.115)	17.001 (1.616)	29%	2.23
Heliothryx barroti	5.142 (0.518)	1.350 (0.178)	13.511 (2.558)	26%	2.63
Klais guimeti	2.585 (0.086)	0.473 (0.030)	7.418 (0.616)	18%	2.87
Lafresnaya lafresnayi	5.240 (0.090)	1.383 (0.031)	16.234 (3.294)	26%	3.10
Lampornis cinereicauda	5.673 (0.191)	1.532 (0.065)	18.157 (1.183)	27%	3.20
Lampornis clemenciae	8.435 (0.205)	2.479 (0.070)	24.635 (0.205)	29%	2.92
Lesbia nuna	4.365 (0.140)	1.083 (0.048)	11.288 (0.518)	25%	2.59
Leucippus chionogaster	4.950 (0.518)	1.284 (0.178)	13.750 (2.558)	26%	2.78
Lophornis delattrei	2.785 (0.075)	0.541 (0.026)	6.977 (0.071)	19%	2.51
Metallura aeneocauda	5.580 (0.172)	1.500 (0.059)	14.171 (0.686)	27%	2.54
Metallura tyrianthina	3.780 (0.063)	0.883 (0.022)	9.795 (0.290)	23%	2.59
Microchera albocoronata	2.632 (0.518)	0.489 (0.178)	5.252 (2.558)	19%	2.00
Ocreatus underwoodii	3.052 (0.038)	0.633 (0.013)	9.994 (0.403)	21%	3.27
Oreonympha nobilis	6.875 (0.342)	1.944 (0.117)	16.488 (0.257)	28%	2.40
Oreotrochilus estella	8.068 (0.520)	2.353 (0.178)	17.979 (0.988)	29%	2.23
Panterpe insignis	5.987 (0.253)	1.640 (0.087)	16.026 (1.015)	27%	2.68
Patagona gigas	22.025 (1.434)	7.141 (0.492)	45.925 (7.446)	32%	2.09
Phaeochroa cuvierii	8.053 (0.567)	2.348 (0.195)	22.340 (2.179)	29%	2.77
Phaethornis guy	5.425 (0.175)	1.447 (0.060)	13.943 (1.903)	27%	2.57
Phaethornis hispidus	5.330 (0.109)	1.414 (0.037)	15.151 (0.614)	27%	2.84
Phaethornis koepckeae	5.256 (0.131)	1.389 (0.045)	14.934 (0.683)	26%	2.84
Phaethornis longuemareus	2.713 (0.078)	0.516 (0.027)	5.780 (0.236)	19%	2.13
Phaethornis malaris	5.363 (0.120)	1.426 (0.041)	15.652 (0.606)	27%	2.92
Phaethornis ruber	2.626 (0.079)	0.487 (0.027)	7.952 (0.420)	19%	3.03
Phaethornis superciliosus	6.612 (0.184)	1.854 (0.063)	16.793 (1.111)	28%	2.54

TABLE 4. *(Continued.)* **Body, muscle parameters of various hummingbird species adapted by [47].**

Schistes geoffroyi	3.673 (0.125)	0.846 (0.043)	10.933 (0.730)	23%	2.98
Selasphorus flammula	2.708 (0.157)	0.515 (0.054)	5.910 (0.321)	19%	2.18
Selasphorus platycercus	3.409 (0.045)	0.755 (0.015)	9.388 (0.204)	22%	2.75
Selasphorus rufus	3.579 (0.060)	0.813 (0.021)	7.971 (0.162)	23%	2.23
Taphrospilus hypostictus	7.080 (0.070)	2.014 (0.024)	23.224 (1.836)	28%	3.28
Thalurania columbica	4.669 (0.104)	1.187 (0.036)	13.254 (0.558)	25%	2.84
Thalurania furcata	4.546 (0.078)	1.145 (0.027)	13.621 (0.466)	25%	3.00
Threnetes niger	6.064 (0.101)	1.666 (0.035)	16.332 (0.684)	27%	2.69
Threnetes ruckeri	5.934 (0.185)	1.621 (0.063)	16.018 (1.091)	27%	2.70

TABLE 5. **Wing parameters of various hummingbird species.**

	Species	m(g)	R(mm)	f(Hz)	$S(mm^2)$	$p_w\ (N/m^2)$	RWL*	AR	k
Hummingbird	Blue-throated[99]	8.4	85	23.3	1763	23.5	11.72	8.2	0.31
	Magnificent[99]	7.4	79	24	1486	24.7	12.78	8.4	0.29
	Black-chinned[99]	3	47	51.2	622.3	23.5	16.71	7.1	0.41
	Rufous[99]	3.3	42	51.7	476.8	33.6	23.24	7.4	0.3
	Rufous [100]	3.2	46.1	-	599.2	36.7	18.12	7.1	-
	Rufous [101]	4.24	45	53.25	494	42.11	26.52	8.2	0.28
		4.24	48	49.1	584	35.61	22.43	7.89	0.31
		4.1	51	47.3	668.5	30.08	19.16	7.78	0.35
		4.54	52	42.57	662.5	33.6	20.70	8.16	0.29
	Anna (male)[102]	4.52	54.5	45.9	714	31.02	19.14	8.32	0.34
	Anna [60]	5.6	50	-	588.2	-	26.81	8.5	-
		5	50	-	543.5	-	26.90	9.2	-
		4.7	59	-	838.8	-	16.73	8.3	-
	Broad-tailed[101]	4.22	55	41.32	780.5	26.52	16.73	7.75	0.35
		3.46	54	36.38	736.5	23.05	15.53	7.92	0.32
		3.66	55	38.71	748	24.01	15.88	8.09	0.34
		5.16	57	39.25	799.5	31.67	18.68	8.13	0.31
		3.6	52	39.53	680.5	25.96	17.26	7.95	0.31
		3.61	56	37.17	817.5	21.66	14.39	7.76	0.35
		3.93	55	38.1	860.5	22.4	14.47	7.03	0.37
		4.1	57	37.94	837.5	24.02	15.29	7.76	0.35
	Ruby-throated (male)[103]	3.58	41	-	460	38.4	25.44	7.34	-
		3.67	41	-	485	37.3	24.53	6.96	-
		4.01	40	-	445	44.1	28.36	7.17	-
		4.16	43	-	455	44.9	28.42	8.13	-
	Ruby-throated (female)[103]	4.36	49	-	635	33.6	21.01	7.55	-
		4.36	48	-	640	33.3	20.85	7.18	-
		4.18	49	-	600	34.2	21.62	8	-
	Amaziliafimbriata[104]	5.1	58.5	35	850	29.4	17.43	8.05	0.29

TABLE 5. ***(Continued.)*** **Wing parameters of various hummingbird species.**

	Aglaiocercuskingismaragdinus[56]	4.65	61.2	21.7	988.9	23.34	14.10	7.58	0.22
	Chrysuroniaoerumejosephine[56]	4.6	54.1	32.8	748	30.35	18.50	7.82	0.25
	Lophomisdelattrei[97]	2.79	40.3	50.7	394.8	34.5	25.10	8.23	0.27
	Phaethornisruber[97]	2.64	40.7	40	484	27.2	19.73	6.83	0.26
	Giant hummingbird (male)[97]	22.6	143	13	4508.4	24	8.87	9.1	0.27
	Giant hummingbird (female) [97]	19.6	139.7	13.9	4307.8	21.5	8.44	8.3	0.3

*The RWL is defined as $RWL = m^{2/3}/A$

TABLE 6. **Artificial wings, including fabrication materials and methods.**

Authors	Model	Wing model(cm) fabrication method	Materials	
			Veins	Membrane
Bontemps et al.[122]	-	MEMS-based	SU-8	Parylene
Roll et al.[123]	-	Cut-and-glue	carbon fibre	Mylar
Watman and Furukawa[124]	-	-	carbon pultrusions	Mylar
Sahai et al. [125]	-	SCM	titanium alloy with carbon fibre reinforcement	Ultra polyester film
Kim et al.[126]	-	Cut-and-glue	graphite/epoxy composite	Flexible PVC
Campolo[127]	Dipteran	Chemical vapour deposition and moulding	carbon fibre	Cellulose acetate film
Wood[128]	Dipteran	SCM	carbon fibre	Mylar
Nguyen et al.[129]	Insects	Cut-and-glue with paper mould	carbon rods	Mylar
Lentink et al[130]	Dragonfly	Cut-and-glue with paper mould	carbon rods	Mylar
Meng et al.[131]	Hoverfly Syrphidae	MEMS-based	SU-8	Polyimide
Tanaka and Wood[132]	Hovering Eristalis	Micro moulding	thermosetting resin	-
Ma et al.[133]	Hovering Eristalis	SCM	carbon fibre	Mylar
Pornisin-Siriak[134]	Bat	MEMS-based	titanium alloy with carbon fibre reinforcement	Parylene
Ho et al.[135]	Cicada	MEMS-based	titanium alloy with carbon fibre reinforcement	Parylene
Keennon et al[39]	Hummingbird	-	carbon fibre	-
Tanaka et al.[135]	Hummingbird	-	carbon fibre-reinforced plastic	Parylene
Coleman et al[42]	Hummingbird	Mold-glue	carbon fibre	1/32 foam membrane
Nan et al.[95]	Hummingbird	Cut-and-glue	carbon fibre	Mylar

REFERENCES

[1] S. Healy and T. A. Hurly, "Hummingbirds," *Current Biol.*, vol. 16, no. 11, pp. 1–2, 2006.

[2] W. Jianghao, Z. Chao, and Z. Yanlai, "Aerodynamic power efficiency comparison of various micro-air-vehicle layouts in hovering flight," *AIAA J.*, vol. 55, no. 4, pp. 1265–1278, 2017.

[3] Y. Bayiz, M. Ghanaatpishe, H. Fathy, and B. Cheng, "Hovering efficiency comparison of rotary and flapping flight for rigid rectangular wings via dimensionless multi-objective optimization," *Bioinspiration Biomimetics*, vol. 13, no. 4, 2018, Art. no. 046002.

[4] T. A. Ward, M. Rezadad, J. C. Fearday, and R. Viyapuri, "A review of biomimetic air vehicle research: 1984–2014," *Int. J. Micro Air Vehicles*, vol. 7, no. 3, pp. 375–394, 2015.

[5] V. M. Mwongera, "A review of flapping wing MAV modelling," *Int. J. Aeronaut. Sci.*, vol. 2, no. 2, p. 17, 2015.

[6] M. F. Platzer, K. D. Jones, J. Young, and J. C. S. Lai, "Flapping wing aerodynamics: Progress and challenges," *AIAA J.*, vol. 46, no. 9, pp. 2136–2149, 2008.

[7] P. Rojratsirikul, "Bio-inspiration in the wings of man-made flyers," *J. Res. Appl. Mech. Eng.*, vol. 1, no. 3, pp. 1–8, 2013.

[8] X. Tan, W. Zhang, X. Ke, W. Chen, C. Zou, W. Liu, F. Cui, X. Wu, and H. Li, "Development of flapping-wing micro air vehicle in Asia," in *Proc. 10th World Congr. Intell. Control Automat.*, Jul. 2012, pp. 3939–3942.

[9] C. Chen and T. Zhang, "A review of design and fabrication of the bionic flapping wing micro air vehicles," *Micromachines*, vol. 10, no. 2, p. 144, 2019.

[10] D. Floreano and R. J. Wood, "Science, technology and the future of small autonomous drones," *Nature*, vol. 521, no. 7553, pp. 460–466, 2015.

[11] R. Dakin, P. S. Segre, A. D. Straw, and D. L. Altshuler, "Morphology, muscle capacity, skill, and maneuvering ability in hummingbirds," *Science*, vol. 359, no. 6376, pp. 653–657, 2018.

[12] P. J. Gullan and P. S. Cranston, *The Insects: An Outline of Entomology*. New York, NY, USA: Wiley, 2005.

[13] R. Dudley, *The Biomechanics of Insect Flight: Form, Function, Evolution*. Princeton, NJ, USA: Princeton Univ. Press, 2002.

[14] C. Zhang and C. Rossi, "A review of compliant transmission mechanisms for bio-inspired flapping-wing micro air vehicles," *Bioinspiration Biomimetics*, vol. 12, no. 2, pp. 1–15, 2017.

[15] C. P. Ellington, "The aerodynamics of hovering insect flight. II. Morphological parameters," *Philos. Trans. Roy. Soc. London B, Biol. Sci.*, vol. 305, no. 1122, pp. 17–40, 1984.

[16] T. Weis-Fogh, "Quick estimates of flight fitness in hovering animals, including novel mechanisms for lift production," *J. Exp. Biol.*, vol. 59, no. 1, pp. 169–230, 1973.

[17] C. van den Berg and C. P. Ellington, "The three–dimensional leading–edge vortex of a 'hovering' model hawkmoth," *Philos. Trans. Roy. Soc. B, Biol. Sci.*, vol. 352, no. 1351, pp. 329–340, 1997.

[18] X. Deng, L. Schenato, W. C. Wu, and S. S. Sastry, "Flapping flight for biomimetic robotic insects: Part I—System modeling," *IEEE Trans. Robot.*, vol. 22, no. 4, pp. 776–788, Aug. 2006.

[19] R. J. Wood, "The first takeoff of a biologically inspired at-scale robotic insect," *IEEE Trans. Robot.*, vol. 24, no. 2, pp. 341–347, Apr. 2008.

[20] H. V. Phan, T. Kang, and H. C. Park, "Design and stable flight of a 21 g insect-like tailless flapping wing micro air vehicle with angular rates feedback control," *Bioinspiration Biomimetics*, vol. 12, no. 3, 2017, Art. no. 036006.

[21] B. Bruggeman, "Improving flight performance of DelFly II in hover by improving wing design and driving mechanism," M.S. thesis, Fac. Aerosp. Eng., Delft Univ. Technol., Delft, The Netherlands, 2010.

[22] Q. V. Nguyen, W.-L. Chan, and M. Debiasi, "Performance tests of a hovering flapping wing micro air vehicle with double wing clap-and-fling mechanism," in *Proc. Int. Micro Air Vehicles Conf. Flight Competition*, 2015, pp. 1–8.

[23] M. Karásek, F. T. Muijres, C. D. Wagter, B. D. W. Remes, and G. C. H. E. de Croon, "A tailless aerial robotic flapper reveals that flies use torque coupling in rapid banked turns," *Science*, vol. 361, no. 6407, pp. 1089–1094, 2018.
[24] X. Q. Bao, A. Bontemps, S. Grondel, and E. Cattan, "Design and fabrication of insect-inspired composite wings for MAV application using MEMS technology," *J. Micromech. Microeng.*, vol. 21, no. 12, 2011, Art. no. 125020.
[25] C. T. Bolsman, J. F. L. Goosen, and F. van Keulen, "Design overview of a resonant wing actuation mechanism for application in flapping wing MAVs," *Int. J. Micro Air. Vehicles*, vol. 1, no. 4, pp. 263–272, 2009.
[26] G.-K. Lau, H.-T. Lim, J.-Y. Teo, and Y.-W. Chin, "Lightweight mechanical amplifiers for rolled dielectric elastomer actuators and their integration with bio-inspired wing flappers," *Smart. Mater. Struct.*, vol. 23, no. 2, 2014, Art. no. 025021.
[27] G.-K. Lau, Y.-W. Chin, and T.-G. La, "Development of elastomeric flight muscles for flapping wing micro air vehicles," *Proc. SPIE, Electroactive Polym. Actuat. Devices*, vol. 10163, Apr. 2017, Art. no. 1016320. doi: 10.1117/12.2260422.
[28] G.-K. Lau, Y.-W. Chin, J. T.-W. Goh, and R. J. Wood, "Dipteran-insect-inspired thoracic mechanism with nonlinear stiffness to save inertial power of flapping-wing flight," *IEEE Trans. Robot.*, vol. 30, no. 5, pp. 1187–1197, Oct. 2014.
[29] K. Meng, W. Zhang, W. Chen, H. Li, P. Chi, C. Zou, X. Wu, F. Cui, W. Liu, and J. Chen, "The design and micromachining of an electromagnetic MEMS flapping-wing micro air vehicle," *Microsyst. Technol.*, vol. 18, no. 1, pp. 127–136, Jan. 2012.
[30] J. Zhang and X. Deng, "Resonance principle for the design of flapping wing micro air vehicles," *IEEE Trans. Robot.*, vol. 33, no. 1, pp. 183–197, Feb. 2017.
[31] D. Warrick, T. Hedrick, M. J. Fernández, B. Tobalske, and A. Biewener, "Hummingbird flight," *Current Biol.*, vol. 22, no. 12, pp. R472–R477, 2012. doi: 10.1016/j.cub.2012.04.057.
[32] F. T. Muijres, L. C. Johansson, R. Barfield, M. Wolf, G. R. Spedding, and A. Hedenström, "Leading-edge vortex improves lift in slow-flying bats," *Science*, vol. 319, no. 5867, pp. 1250–1253, 2008.
[33] B. Tobalske and K. Dial, "Flight kinematics of black-billed magpies and pigeons over a wide range of speeds," *J. Exp. Biol.*, vol. 199, no. 2, pp. 263–280, 1996.
[34] K. P. Dial, A. A. Biewener, B. W. Tobalske, and D. R. Warrick, "Mechanical power output of bird flight," *Nature*, vol. 390, no. 6655, pp. 67–70, 1997.
[35] U. M. L. Norberg, "Structure, form, and function of flight in engineering and the living world," *J. Morphol.*, vol. 252, no. 1, pp. 52–81, 2002.
[36] A. Azuma, *The Biokinetics of Flying and Swimming* (AIAA Education Series). 2nd ed. Washington, DC, USA: AIAA, 2006.
[37] C. H. Greenewalt, *Hummingbirds*. New York, NY, USA: Dover, 1990.
[38] R. T. Peterson, *The Birds*. New York, NY, USA: Time Inc., 1968.
[39] M. T. Keennon, K. Klingebiel, and H. Won, "Development of the nano hummingbird: A tailless flapping wing micro air vehicle," in *Proc. AIAA*, 2012, p. 588.
[40] R. Leys, D. Reynaerts, and D. Vandepitte, "Outperforming hummingbirdsâĂŹ load-lifting capability with a lightweight hummingbird-like flapping-wing mechanism," *Biol. Open*, vol. 5, no. 8, pp. 1052–1060, 2016.
[41] J. Zhang, F. Fei, Z. Tu, and X. Deng, "Design optimization and system integration of robotic hummingbird," in *Proc. IEEE Int. Conf. Robot. Autom. (ICRA)*, May/Jun. 2017, pp. 5422–5428.
[42] D. Coleman, M. Benedict, V. Hrishikeshavan, and I. Chopra, "Design, development and flight-testing of a robotic hummingbird," in *Proc. AHS 71st Annu. Forum*, Virginia Beach, VA, USA, 2015, pp. 1–18.
[43] M. Karásek, Y. H. Nan, I. Romanescu, and A. Preumont, "Pitch moment generation and measurement in a robotic hummingbird," *Int. J. Micro Air Vehicles*, vol. 5, pp. 299–310, Dec. 2013.
[44] D. L. Altshuler and R. Dudley, "The ecological and evolutionary interface of hummingbird flight physiology," *J. Exp. Biol.*, vol. 205, no. 16, pp. 2325–2336, 2002.
[45] S. Mahalingam and K. C. Welch, Jr., "Neuromuscular control of hovering wingbeat kinematics in response to distinct flight challenges in the ruby-throated hummingbird, *Archilochus colubris*," *J. Exp. Biol.*, vol. 216, no. 22, pp. 4161–4171, 2013.
[46] K. C. Welch, Jr., and D. L. Altshuler, "Fiber type homogeneity of the flight musculature in small birds," *Comparative Biochem. Physiol. B, Biochem. Mol. Biol.*, vol. 152, no. 4, pp. 324–331, Apr. 2009.
[47] D. L. Altshuler, R. Dudley, S. M. Heredia, and J. A. McGuire, "Allometry of hummingbird lifting performance," *J. Exp. Biol.*, vol. 213, no. 5, pp. 725–734, 2010.
[48] E. L. Brainerd, D. B. Baier, S. M. Gatesy, T. L. Hedrick, K. A. Metzger, S. L. Gilbert, and J. J. Crisco, "X-ray reconstruction of moving morphology (XROMM): Precision, accuracy and applications in comparative biomechanics research," *J. Exp. Zool. A, Ecol. Genet. Physiol.*, vol. 313A, pp. 262–279, Jun. 2010.
[49] K. P. Dial, "Avian forelimb muscles and nonsteady flight: Can birds fly without using the muscles in their wings?" *Auk*, vol. 109, no. 4, pp. 874–885, 1992.
[50] T. L. Hedrick, B. W. Tobalske, I. G. Ros, D. R. Warrick, and A. A. Biewener, "Morphological and kinematic basis of the hummingbird flight stroke: Scaling of flight muscle transmission ratio," *Proc. Roy. Soc. Lond. B, Biol. Sci.*, vol. 279, pp. 1986–1992, Dec. 2011.
[51] A. Roshanbin, H. Altartouri, M. Karásek, and A. Preumont, "COLIBRI: A hovering flapping twin-wing robot," *Int. J. Mirco Air Vehicles*, vol. 9, no. 4, pp. 270–282, 2017.
[52] Y. Nan, B. Peng, Y. Chen, Z. Feng, and D. McGlinchey, "Comparison study on flapping mechanisms of flapping wing micro air vehicle characterized on hovering flight," in *Proc. 2nd Int. Conf. Service Robot. Technol.*, 2019, pp. 1–6.
[53] J. W. Gerdes, S. K. Gupta, and S. Wilkerson, "A review of bird-inspired flapping wing miniature air vehicle designs," *J. Mech. Robot.*, vol. 4, no. 2, 2012, Art. no. 021003.
[54] C. Zhang and C. Rossi, "Effects of elastic hinges on input torque requirements for a motorized indirect-driven flapping-wing compliant transmission mechanism," *IEEE Access*, vol. 7, pp. 13068–13077, 2019.
[55] M. Stolpe and K. Zimmer, "Der Schwirrflug des Kolibri im Zeitlupenfilm," *J. Ornithol.*, vol. 87, no. 1, pp. 136–155, 1939.
[56] T. Weis-Fogh, "Energetics of hovering flight in hummingbirds and in Drosophila," *J. Exp. Biol.*, vol. 56, no. 1, pp. 79–104, 1972.
[57] U. M. Norberg, *Vertebrate Flight: Mechanics, Physiology, Morphology, Ecology and Evolution*. Berlin, Germany: Springer, 1990.
[58] M. Karásek and A. Preumont, "Flapping flight stability in hover: A comparison of various aerodynamic models," *Int. J. Micro Air Vehicles*, vol. 4, no. 3, pp. 203–226, 2012.
[59] V. M. Ortega-Jimenez, N. Sapir, M. Wolf, E. A. Variano, and R. Dudley, "Into turbulent air: Size-dependent effects of von Kármán vortex streets on hummingbird flight kinematics and energetics," *Proc. Roy. Soc. B, Biol. Sci.*, vol. 281, pp. 2–21, May 2014.
[60] C. H. Greenewalt, "The wings of insects and birds as mechanical oscillators," *Proc. Amer. Philos. Soc.*, vol. 104, no. 6, pp. 605–611, 1960.
[61] D. R. Warrick, B. W. Tobalske, and D. R. Powers, "Aerodynamics of the hovering hummingbird," *Nature*, vol. 435, pp. 1094–1097, Jun. 2005.
[62] M. Wolf, V. M. Ortega-Jimenez, and R. Dudley, "Structure of the vortex wake in hovering Anna's hummingbirds (*Calypte anna*)," *Proc. Roy. Soc. B, Biol. Sci.*, vol. 280, Dec. 2013, Art. no. 20132391.
[63] C. van den Berg and C. P. Ellington, "The vortex wake of a 'hovering' model hawkmoth," *Philos. Trans. Roy. Soc. B, Biol. Sci.*, vol. 352, pp. 329–340, Mar. 1997.
[64] R. J. Wootton, "Geometry and mechanics of insect hindwing fans: A modelling approach," *Proc. Roy. Soc. Lond. B, Biol. Sci.*, vol. 262, pp. 181–187, Nov. 1995.
[65] S. A. Combes and T. L. Daniel, "Into thin air: Contributions of aerodynamic and inertial-elastic forces to wing bending in the hawkmoth *Manduca sexta*," *J. Exp. Biol.*, vol. 206, no. 17, pp. 2999–3006, 2003.
[66] A. P. Willmott, C. P. Ellington, and A. L. R. Thomas, "Flow visualization and unsteady aerodynamics in the flight of the hawkmoth, *Manduca sexta*," *Philos. Trans. Roy. Soc. Lond. B, Biol. Sci.*, vol. 352, pp. 303–316, Mar. 1997.
[67] C. P. Ellington, C. van den Berg, A. P. Willmott, and A. L. R. Thomas, "Leading-edge vortices in insect flight," *Nature*, vol. 384, pp. 626–630, Dec. 1996.
[68] M. H. Dickinson, F.-O. Lehmann, and S. P. Sane, "Wing rotation and the aerodynamic basis of insect flight," *Science*, vol. 284, no. 5422, pp. 1954–1960, 1999.
[69] R. D. Warrick, B. W. Tobalske, D. R. Powers, and M. H. Dickenson, "The aerodynamics of hummingbird flight," Dept. Biol. Chem., George Fox Univ., Newberg, OR, USA, Tech. Rep., 2007, pp. 1–5. [Online]. Available: https://arc.aiaa.org/doi/abs/10.2514/6.2007-41
[70] D. D. Chin and D. Lentink, "Flapping wing aerodynamics: From insects to vertebrates," *J. Exp. Biol.*, vol. 219, no. 7, pp. 920–932, 2016.

[71] J. M. Wakeling and C. P. Ellington, "Dragonfly flight. II. Velocities, accelerations and kinematics of flapping flight," *J. Exp. Biol.*, vol. 200, no. 3, pp. 557–582, 1997.

[72] D. R. Warrick, B. W. Tobalske, and D. R. Powers, "Lift production in the hovering hummingbird," *Proc. Roy. Soc. B, Biol. Sci.*, vol. 276, pp. 3747–3752, Aug. 2009.

[73] F. T. Muijres, L. C. Johansson, and A. Hedenström, "Leading edge vortex in a slow-flying passerine," *Biol. Lett.*, vol. 8, no. 4, pp. 554–557, 2012.

[74] J. M. Birch, W. B. Dickson, and M. H. Dickinson, "Force production and flow structure of the leading edge vortex on flapping wings at high and low Reynolds numbers," *J. Exp. Biol.*, vol. 207, no. 7, pp. 1063–1072, 2004.

[75] F.-O. Lehmann, "The mechanisms of lift enhancement in insect flight," *Naturwissenschaften*, vol. 91, no. 3, pp. 101–122, 2004.

[76] C. Ellington, "Insects versus birds: The great divide (invited)," in *Proc. 44th AIAA Aerosp. Sci. Meeting Exhibit*, vol. 35, 2006, pp. 1–6.

[77] D. E. Rival, J. Kriegseis, P. Schaub, A. Widmann, and C. Tropea, "Characteristic length scales for vortex detachment on plunging profiles with varying leading-edge geometry," *Exp. Fluids*, vol. 55, no. 1, p. 1660, 2014.

[78] A. Hedenström, L. C. Johansson, M. Wolf, R. von Busse, Y. Winter, and G. R. Spedding, "Bat flight generates complex aerodynamic tracks," *Science*, vol. 316, no. 5826, pp. 894–897, 2007.

[79] S. Pournazeri, P. S. Segre, M. Princevac, and D. L. Altshuler, "Hummingbirds generate bilateral vortex loops during hovering: Evidence from flow visualization," *Exp. Fluids.*, vol. 54, pp. 1439–1450, Jan. 2013.

[80] A. Roshanbin and A. Preumont, "Yaw control torque generation for a hovering robotic hummingbird," *Int. J. Adv. Robot. Syst.*, vol. 16, no. 1, 2019, Art. no. 1729881418823968.

[81] Y. Nan, B. Peng, Y. Chen, Z. Feng, and D. McGlinchey, "Can scalable design of wings for flapping wing micro air vehicle be inspired by natural flyers?" *Int. J. Aerosp. Eng.*, vol. 2018, Oct. 2018, Art. no. 9538328.

[82] R. Å. Norberg and U. M. Norberg, "Take-off, landing, and flight speed during fishing flights of Gavia stellata (Pont.)," *OrnisScandinavica*, vol. 2, no. 1, pp. 55–67, 1971.

[83] H. I. Fisher, "Bony mechanism of automatic flexion and extension in the Pigeon's wing," *Science*, vol. 126, no. 3271, p. 446, 1957.

[84] T. L. Hedrick, "Software techniques for two- and three-dimensional kinematic measurements of biological and biomimetic systems," *Bioinspiration Biomimetics*, vol. 3, no. 3, 2008, Art. no. 34001.

[85] S. M. Gatesy, D. B. Baier, F. A. Jenkins, and K. P. Dial, "Scientific rotoscoping: A morphology-based method of 3-D motion analysis and visualization," *J. Exp. Zool. A, Ecol. Genet. Physiol.*, vol. 313A, no. 5, pp. 244–261, 2010.

[86] A. J. Bergou, S. Xu, and Z. J. Wang, "Passive wing pitch reversal in insect flight," *J. Fluid Mech.*, vol. 591, pp. 321–337, Nov. 2007.

[87] U. M. Norberg, "Energetics of flight," in *Avian Energetics and Nutritional Ecology*, C. Carey, Ed. New York, NY, USA: Chapman & Hall, 1996, pp. 199–249.

[88] L. Prandtl and O. K. G. Tietjens, *Applied Hydro- and Aeromechanics: Based on Lectures of L. Prandtl*, vol. 2. Mineola, NY, USA: Dover, 1957.

[89] W. Z. Stepniewski, *Rotary-Wing Aerodynamics*. Mineola, NY, USA: Dover, 1984.

[90] N. Phillips, K. Knowles, and R. J. Bomphrey, "The effect of aspect ratio on the leading-edge vortex over an insect-like flapping wing," *Bioinspiration Biomimetics*, vol. 10, no. 5, pp. 1–18, 2015.

[91] J. R. Usherwood and C. P. Ellington, "The aerodynamics of revolving wings II. Propeller force coefficients from mayfly to quail," *J. Exp. Biol.*, vol. 205, no. 11, pp. 1565–1576, 2002.

[92] Y. J. Lee, K. B. Lua, and T. T. Lim, "Aspect ratio effects on revolving wings with Rossby number consideration," *Bioinspiration Biomimetics*, vol. 11, no. 5, 2016, Art. no. 056013.

[93] G. Luo and M. Sun, "The effects of corrugation and wing planform on the aerodynamic force production of sweeping model insect wings," *Acta Mech. Sinica*, vol. 21, no. 6, pp. 531–541, Dec. 2005.

[94] U. M. Norberg and R. A. Norberg, "Ecomorphology of flight and tree-trunk climbing in birds," in *Proc. Acta 19th Congressus Internationalis Ornithologici*, vol. 2, 1988, pp. 2271–2282.

[95] H. C. Corben, "Wing-beat frequencies, wing-areas and masses of flying insects and hummingbirds," *J. Exp. Biol.*, vol. 102, no. 4, pp. 611–623, Jun. 1983.

[96] Y. Nan, M. Karásek, M. Lalami, and A. Preumont, "Experimental optimization of wing shape for a hummingbird-like flapping wing micro air vehicle," *Bioinspiration Biomimetics*, vol. 12, no. 2, pp. 1–16, 2017.

[97] D. L. Altshuler, "Ecophysiology of hummingbird flight along elevational gradients: An integrated approach," Ph.D. dissertation, Dept. Biol. Sci., Univ. Texas Austin, Austin, TX, USA, 2001.

[98] J. W. Kruyt, E. M. Quicazán-Rubio, G. F. van Heijst, D. L. Altshuler, and D. Lentink, "Hummingbird wing efficacy depends on aspect ratio and compares with helicopter rotors," *J. Roy Soc. Interface*, vol. 11, no. 3, pp. 570–581, 2014.

[99] M. J. Fernandez, "Flight performance and comparative energetics of the giant Andean hummingbird," Ph.D. dissertation, Dept. Integrative Biol. Museum Vertebrate Zoology, Univ. California, Berkeley, Berkeley, CA, USA, 2010.

[100] P. Chai and D. Miliard, "Flight and side constraints: Hovering performance of large hummingbirds under maximal loading," *J. Exp. Biol.*, vol. 200, no. 21, pp. 2757–2763, 1997.

[101] B. W. Tobalske, D. L. Altshuler, and D. R. Powers, "Take-off mechanics in hummingbirds (Trochilidae)," *J. Exp. Biol.*, vol. 207, no. 8, pp. 1345–1352, 2004.

[102] D. J. Wells, "Muscle performance in hovering hummingbirds," *J. Exp. Biol.*, vol. 178, no. 1, pp. 39–57, 1993.

[103] D. Evangelista, M. J. Fernández, M. S. Berns, A. Hoove, and R. Dudley, "Hovering energetics and thermal balance in Anna's hummingbirds (*Calypte anna*)," *Physiol. Biochem. Zool.*, vol. 83, no. 3, pp. 406–413, 2010.

[104] P. Chai, R. Harrykissoon, and R. Dudley, "Hummingbird hovering performance in hyperoxic heliox: Effects of body mass and sex," *J. Exp. Biol.*, vol. 199, no. 12, pp. 2745–2755, 1996.

[105] U. M. Norberg, "Flight and scaling of flyers in nature," *WIT Trans. State Art Sci. Eng.*, vol. 3, pp. 120–154, 2006. [Online]. Available: https://www.witpress.com/Secure/elibrary/papers/1845640012/1845640012204FU1.pdf. doi: 10.2495/1-84564-001-2/2d.

[106] A. L. R. Thomas, "On the aerodynamics of birds' tails," *Philos. Trans. Roy. Soc. B, Biol. Sci.*, vol. 340, pp. 361–380, Jun. 1993.

[107] M. Andersson, "Female choice selects for extreme tail length in a widowbird," *Nature*, vol. 299, pp. 818–820, Oct. 1982.

[108] J. C. Clark, "The evolution of tail shape in hummingbirds," *Auk*, vol. 127, no. 1, pp. 44–56, 2010.

[109] V. A. Tucker, "Pitching equilibrium, wing span and tail span in a gliding harris' Hawk, *Parabuteo Unicinctus*," *J. Exp. Biol.*, vol. 165, no. 1, pp. 21–43, 1992.

[110] R. Å. Norberg, "Swallow tail streamer is a mechanical device for self-deflection of tail leading edge, enhancing aerodynamic efficiency and flight manoeuvrability," *Philos. Trans. Roy. Soc. B, Biol. Sci.*, vol. 257, pp. 227–233, Sep. 1994.

[111] A. L. R. Thomas and A. Balmford, "How natural selection shapes birds' tails," *Amer. Naturalist*, vol. 146, no. 6, pp. 848–868, 1995.

[112] W. J. Maybury, J. M. V. Rayner, and L. B. Couldrick, "Lift generation by the avian tail," *Proc. Roy. Soc. B, Biol. Sci.*, vol. 268, no. 1475, pp. 1443–1448, 2001.

[113] T. L. Hedrick, B. Cheng, and X. Deng, "Wingbeat time and the scaling of passive rotational damping in flapping flight," *Science*, vol. 324, no. 5924, pp. 252–255, 2009.

[114] D. L. Altshuler, E. M. Quicazán-Rubio, P. S. Segre, and K. M. Middleton, "Wingbeat kinematics and motor control of yaw turns in Anna's hummingbirds (*Calypte anna*)," *J. Exp. Biol.*, vol. 215, no. 23, pp. 4070–4084, 2012.

[115] N. F. Steven, R. Sayaman, and M. H. Dickinson, "The aerodynamics of free-flight maneuvers in Drosophila," *Science*, vol. 300, no. 5618, pp. 495–498, Apr. 2003.

[116] S. Ravi, J. D. Crall, L. McNeilly, S. F. Gagliardi, A. A. Biewener, and S. A. Combes, "Hummingbird flight stability and control in freestream turbulent winds," *J. Exp. Biol.*, vol. 218, no. 9, pp. 1444–1452, 2015.

[117] H. Altartouri, A. Roshanbin, G. Andreolli, L. Fazzi, M. Karasek, and A. Preumont, "Passive stability enhancement with sails of a hovering flapping twin-wing robot," *Int. J. Micro Air Vehicles*, vol. 11, pp. 1–9, Apr. 2019.

[118] G. Sachs, "Tail effects on yaw stability in birds," *J. Theor. Biol.*, vol. 249, no. 3, pp. 464–472, 2007.

[119] Y. H. Nan and Y. Chen, "Tail study of hummingbird-like robot," Ind. 4.0 Artif. Intell. Lab., Dongguan, China. Tech. Rep. 20190728, 2019.

[120] M. Karásek, A. Hua, Y. H. Nan, M. Lalami, and A. Preumont, "Pitch and roll control mechanism for a hovering flapping wing MAV," *Int. J. Micro Air Vehicles*, vol. 6, no. 4, pp. 253–264, 2014.

[121] A. Bontemps, T. Vanneste, J.-B. Paquet, T. Dietsch, S. Grondel, and E. Cattan, "Design and performance of an insect-inspired nano air vehicle," *Smart Mater. Struct.*, vol. 22, no. 1, 2013, Art. no. 14008.

[122] J. A. Roll, B. Cheng, and X. Deng, "Design, fabrication, and experiments of an electromagnetic actuator for flapping wing micro air vehicles," in *Proc. IEEE Int. Conf. Robot. Autom.*, May 2013, pp. 809–815.

[123] D. Watman and T. Furukawa, "A parametric study of flapping wing performance using a robotic flapping wing," in *Proc. IEEE Int. Conf. Robot. Autom.*, May 2009, pp. 3638–3643.
[124] R. Sahai, K. C. Galloway, and R. J. Wood, "Elastic element integration for improved flapping-wing micro air vehicle performance," *IEEE Trans. Robot.*, vol. 29, no. 1, pp. 32–41, Feb. 2013.
[125] D.-K. Kim, H.-I. Kim, J.-H. Han, and K.-J. Kwon, "Experimental investigation on the aerodynamic characteristics of a bio-mimetic flapping wing with macro-fiber composites," *J. Intell. Mater. Syst. Struct.*, vol. 19, pp. 423–431, Oct. 2007.
[126] D. Campolo, M. Azhar, G.-K. Lau, and M. Sitti, "Can DC motors directly drive flapping wings at high frequency and large wing strokes?" *IEEE/ASME Trans. Mechatronics*, vol. 19, no. 1, pp. 109–120, Feb. 2014.
[127] R. J. Wood, "Design, fabrication, and analysis of a 3DOF, 3 cm flapping-wing MAV," in *Proc. IEEE Int. Conf. Intell. Robots Syst.*, Oct./Nov. 2007, pp. 1576–1581.
[128] Q.-V. Nguyen, W. L. Chan, and M. Debiasi, "An insect-inspired flapping wing micro air vehicle with double wing clap-fling effects and capability of sustained hovering," *Proc. SPIE*, vol. 9429, Mar. 2015, Art. no. 94290U.
[129] D. Lentink, S. R. Jongerius, and N. L. Bradshaw, "The scalable design of flapping micro-air vehicles inspired by insect flight," in *Flying Insects and Robots*. Cham, Switzerland: Springer, 2010, pp. 185–205.
[130] H. Tanaka and R. J. Wood, "Fabrication of corrugated artificial insect wings using laser micromachined molds," *J. Micromech. Microeng.*, vol. 20, no. 7, 2010, Art. no. 75008.
[131] K. Y. Ma, P. Chirarattananon, S. B. Fuller, and R. J. Wood, "Controlled flight of a biologically inspired, insect-scale robot," *Science*, vol. 340, no. 6132, pp. 603–607, 2013.
[132] T. N. Pornsin-Sirirak, Y.-C. Tai, C.-M. Ho, and M. Keennon, "Microbat: A palm-sized electrically powered ornithopter," in *Proc. NASA/JPL Work. Biomorphic Robot.*, 2001, pp. 1–13.
[133] S. Ho, H. Nassef, N. Pornsinsirirak, Y.-C. Tai, and C.-M. Ho, "Unsteady aerodynamics and flow control for flapping wing flyers," *Prog. Aerosp. Sci.*, vol. 39, no. 8, pp. 635–681, Nov. 2003.
[134] H. Tanaka, H. Okada, Y. Shimasue, and H. Liu, "Flexible flapping wings with self-organized microwrinkles," *Bioinspiration Biomimetics*, vol. 10, no. 4, 2015, Art. no. 46005.
[135] Y. Chen, Z. Song, G. Zhang, M. T. Majeed, and Y. Li, "Spatio-temporal evolutionary analysis of the township enterprises of Beijing suburbs using computational intelligence assisted design framework," *Palgrave Commun.*, vol. 4, Mar. 2018, Art. no. 31.
[136] Y. Chen and Y. Li, *Computational Intelligence Assisted Design* (In the Era of Industry 4.0). Boca Raton, FL, USA: CRC Press, 2018.
[137] Y. Chen, X. Wang, Z. Sha, and S. Wu, "Uncertainty analysis for multistate weighted behaviours of rural area with carbon dioxide emission estimation," *Appl. Soft Comput.*, vol. 12, no. 8, pp. 2631–2637, 2012,".
[138] Y. Chen and Y. Li, "Intelligent autonomous pollination for future farming - a micro air vehicle conceptual framework with artificial intelligence and human-in-the-loop," *IEEE Access*, vol. 7, pp. 119706–119717, 2019. doi: 10.1109/ACCESS.2019.2937171.
[139] Z. Wang, X. Cheng, and J. Liu, "Time-dependent concurrent reliability-based design optimization integrating experiment-based model validation," *Struct. Multidisciplinary Optim.*, vol. 57, no. 4, pp. 1523–1531, Apr. 2018.
[140] S. Yu, Z. Wang, and K. Zhang, "Sequential time-dependent reliability analysis for the lower extremity exoskeleton under uncertainty," *Rel. Eng. Syst. Saf.*, vol. 170, pp. 45–52, Feb. 2018.
[141] S. Yu and Z. Wang, "A novel time-variant reliability analysis method based on failure processes decomposition for dynamic uncertain structures," *ASME J. Mech. Design*, vol. 140, no. 5, 2018, Art. no. 051401.
[142] S. Yu, Z. Wang, and D. Meng, "Time-variant reliability assessment for multiple failure modes and temporal parameters," *Struct. Multidisciplinary Optim.*, vol. 58, no. 4, pp. 1705–1717, Oct. 2018.
[143] Z. Wang, S. Yu, L. Y. Chen, and Y. Li, "Robust design for the lower extremity exoskeleton under a stochastic terrain by mimicking wolf pack behaviors," *IEEE Access*, vol. 6, pp. 30714–30725, 2018.
[144] Z. Wang, Z. Wang, S. Yu, and K. Zhang, "Time-dependent mechanism reliability analysis based on envelope function and vine-copula function," *Mech. Mach. Theory*, vol. 134, pp. 667–684, Apr. 2019.

YANGHAI NAN received the B.S. degree in mechanical engineering from Yanbian University, in 2006, and the M.S. degree in mechanical engineering from Chonnam National University, in 2008. His research interests mainly include robotics and applications.

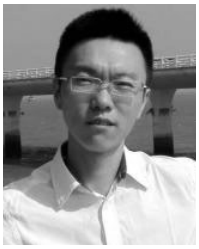

BEI PENG received the B.S. degree from Tsinghua University, in 1999, and the M.S. and Ph.D. degrees from Northwestern University, in 2003 and 2008, respectively. He is currently a Full Professor of mechatronics engineering with the University of Electronic Science and Technology of China. He holds 30 authorized patents. He has served as a PI or a Co-PI for over ten research projects, including the National Science Foundation of China (NSFC). He has published over 100 journal and conference articles. His research interests mainly include intelligent manufacturing systems, nano material design, and its applications.

YI CHEN (M'10–SM'17) received the B.Sc. degree in automotive engineering from the Chongqing University of Technology, in 2000, the M.Sc. degree in automotive engineering from Chongqing University, in 2004, and the Ph.D. degree in mechanical engineering from the University of Glasgow, in 2010. He is also a chartered engineer. He has a high-level output of research publications in leading international journals and presentations at international conferences, which related to the research areas of robotics, digital manufacturing, and industry 4.0, which demonstrates significant research and grant potential in engineering and cross-disciplinary applications. He has published more than 100 academic articles in both high-impact international academic journals and international conferences. He has also been actively involved in both academic research and KTP projects as a PI and a Co-PI funded by EPSRC, U.K., Horizon 2020 (EU), NSFC, China, the National Key Research and Development Program of China, and industrial funding bodies. He is a member of IET, AAAI, AIAA, and ASME, and a Fellow of HEA and IMechE. He is one of the co-organizers of the WCCI 2016 Special Session on Computational Intelligence for Industry 4.0 and the CEC 2019 Special Session on Evolutionary Computation for Creativity, Manufacture and Engineering Management in the Industry 4.0 Era. He has been selected as a Publons' top 1% of reviewers in computer science and engineering. He is an editorial board member. He has been a Guest Editor of five special issues.

DON MCGLINCHEY received the Ph.D. degree in particle technology. He has undertaken consultancy projects for both multinational companies and small to medium enterprises (SME's), and delivered short courses in Europe, USA, and U.K. He is currently a Professor with the Department of Mechanical Engineering, Glasgow Caledonian University, where he is a Leader of the Engineering Simulation and Advanced Manufacturing Research Group. He is also an academic of international standing within the particulate solids handling community. He is also a chartered physicist with a Ph.D. degree in the particle technology area. He has authored over 50 research articles. His current research interests include multiphase flow pipeline transport measurement and modeling, and the application of machine learning to engineering systems in the context of Industry 4.0. He is the Editor of two books.